

Review

Capture-SELEX: Selection Strategy, Aptamer Identification, and Biosensing Application

Sin Yu Lam ¹, Hill Lam Lau ¹ and Chun Kit Kwok ^{1,2,*}

¹ State Key Laboratory of Marine Pollution and Department of Chemistry, City University of Hong Kong, Hong Kong SAR 999077, China

² Shenzhen Research Institute, City University of Hong Kong, Shenzhen 518057, China

* Correspondence: ckkwok42@cityu.edu.hk

Abstract: Small-molecule contaminants, such as antibiotics, pesticides, and plasticizers, have emerged as one of the substances most detrimental to human health and the environment. Therefore, it is crucial to develop low-cost, user-friendly, and portable biosensors capable of rapidly detecting these contaminants. Antibodies have traditionally been used as biorecognition elements. However, aptamers have recently been applied as biorecognition elements in aptamer-based biosensors, also known as aptasensors. The systematic evolution of ligands by exponential enrichment (SELEX) is an *in vitro* technique used to generate aptamers that bind their targets with high affinity and specificity. Over the past decade, a modified SELEX method known as Capture-SELEX has been widely used to generate DNA or RNA aptamers that bind small molecules. In this review, we summarize the recent strategies used for Capture-SELEX, describe the methods commonly used for detecting and characterizing small-molecule-aptamer interactions, and discuss the development of aptamer-based biosensors for various applications. We also discuss the challenges of the Capture-SELEX platform and biosensor development and the possibilities for their future application.

Keywords: nucleic acid aptamer; DNA and RNA Capture-SELEX; small molecule contaminant; characterization; aptamer; biosensing applications



Citation: Lam, S.Y.; Lau, H.L.; Kwok, C.K. Capture-SELEX: Selection Strategy, Aptamer Identification, and Biosensing Application. *Biosensors* **2022**, *12*, 1142. <https://doi.org/10.3390/bios12121142>

Received: 5 November 2022

Accepted: 29 November 2022

Published: 7 December 2022

Publisher's Note: MDPI stays neutral with regard to jurisdictional claims in published maps and institutional affiliations.



Copyright: © 2022 by the authors. Licensee MDPI, Basel, Switzerland. This article is an open access article distributed under the terms and conditions of the Creative Commons Attribution (CC BY) license (<https://creativecommons.org/licenses/by/4.0/>).

1. Introduction

Accumulating evidence suggests that small-molecule contaminants, such as antibiotics, pesticides, and plasticizers, pose a severe threat to human health and the environment worldwide. Antibiotics have been extensively used for decades to treat bacterial infections, and most are recalcitrant to biodegradation and elimination [1]. Moreover, the global overuse of antibiotics has led to their long-term persistence in the marine environment. More than 700,000 human deaths per year are attributable to bacterial resistance to antimicrobials (including antibiotics), with this number projected to increase to 10 million by 2050 [2]. Pesticides are widely used in agriculture to control pests and disease carriers. According to the World Health Organization, 193,460 unintentional deaths in 2012 were due to pesticide poisoning [3]. Plasticizers are widely applied in plastic products, such as Di(2-ethylhexyl)phthalate (DEHP), contaminating the environment. Toxic plasticizers with their toxicological effects, including endocrine disruption, carcinogenicity, and bioaccumulation potential [4–6], may enter human body via inhalation, ingestion, and dermal contact, reflecting the high risk of harm to human health.

Some traditional techniques for detecting small-molecule contaminants with high accuracy include high-performance liquid chromatography [7,8], enzyme-linked immunosorbent assays [9,10], and liquid chromatography–mass spectrometry [11,12]. However, these techniques are costly and laborious, and can only be performed by professional technicians. Therefore, there is an urgent need for robust aptamer-based biosensors (also called aptasensors), for low-cost, user-friendly, and rapid detection of small-molecule contaminants.

Aptamers are short, single-stranded DNA or RNA oligonucleotides that are able to bind its target with high affinity and specificity. The development of an aptasensor for detecting small-molecule contaminants requires the generation of a novel aptamer. It has gradually replaced traditional antibodies in some applications as they have several advantages over antibodies, such as thermal stability, low cost, amenability to chemical modification, and ease of generation [13,14]. Furthermore, when designed appropriately, the chemical modification of aptamers often does not affect—and sometimes even strengthens—their binding affinity for their targets, whereas the chemical modification of antibodies may remove their affinity for their targets [13]. Moreover, antibodies can only bind to a narrow range of targets, such as immunogenic non-toxic molecules and other molecules that do not cause strong immune responses [13]. In contrast, aptamers can selectively and tightly bind to a broad range of targets, including proteins [15–17], cells [18,19], microorganisms [20], and small-molecule contaminants [21–24], which may be either immunogenic or non-immunogenic. In addition, the *in vivo* generation of antibodies is a lengthy process (~6 months or longer) and requires a living host, whereas aptamers can be generated through *in vitro* selection (~2–8 weeks) using a method known as systematic evolution of ligands by exponential enrichment (SELEX) [13].

Three research groups independently developed the first SELEX method and all reported their findings in 1990: Tuerk and Gold [25], Ellington and Szostak [26], and Joyce [27]. Since then, many derivative methods of SELEX have been developed, such as capillary electrophoresis (CE)-SELEX [28–30], graphene oxide (GO)-SELEX [31–33], cell-SELEX [34–36], *in vivo* SELEX [37,38], and Capture-SELEX [22,23,39]. Capture-SELEX selects DNA or RNA aptamers that bind small-molecule contaminants and is partly based on FluMag-SELEX. Stoltenburg et al. reported FluMag-SELEX in 2005 [40], and it is based on the magnetic bead (MB)-based SELEX, whereby the fluorescein-labeled oligonucleotides is to monitor the enrichment of target-specific aptamers with the quantification in each round, and biotinylated target molecules are immobilized onto the surface of streptavidin-coated magnetic beads (SA-MBs). However, it is more challenging to immobilize biotinylated small-molecule targets than biotinylated large-molecule targets such as proteins [41], as small-molecule targets have fewer functional groups. Thus, Capture-SELEX is an effective alternative to FluMag-SELEX, as Capture-SELEX involves the immobilization of a biotinylated hybridized library on a solid support, which is more feasible than the immobilization of biotinylated targets on a solid support (Figure 1). Due to the differences in the principle, Capture-SELEX also has some deficiencies compared to other SELEX methods [41]. The false-positive may happen in the immobilization process of Capture-SELEX. The complemented library may have a dynamic dissociation equilibrium due to the weak force, and some unbound sequences (non-biotinylated) are also dissociated from the solid support. Moreover, conformational changes of the target are essential for the success of aptamer screening and diversity in the selection process. This review discusses Capture-SELEX-based selection strategies for small-molecule contaminant targets, methods used to identify and characterize small molecule–aptamer interactions, and biosensing applications of aptamers generated using Capture-SELEX.

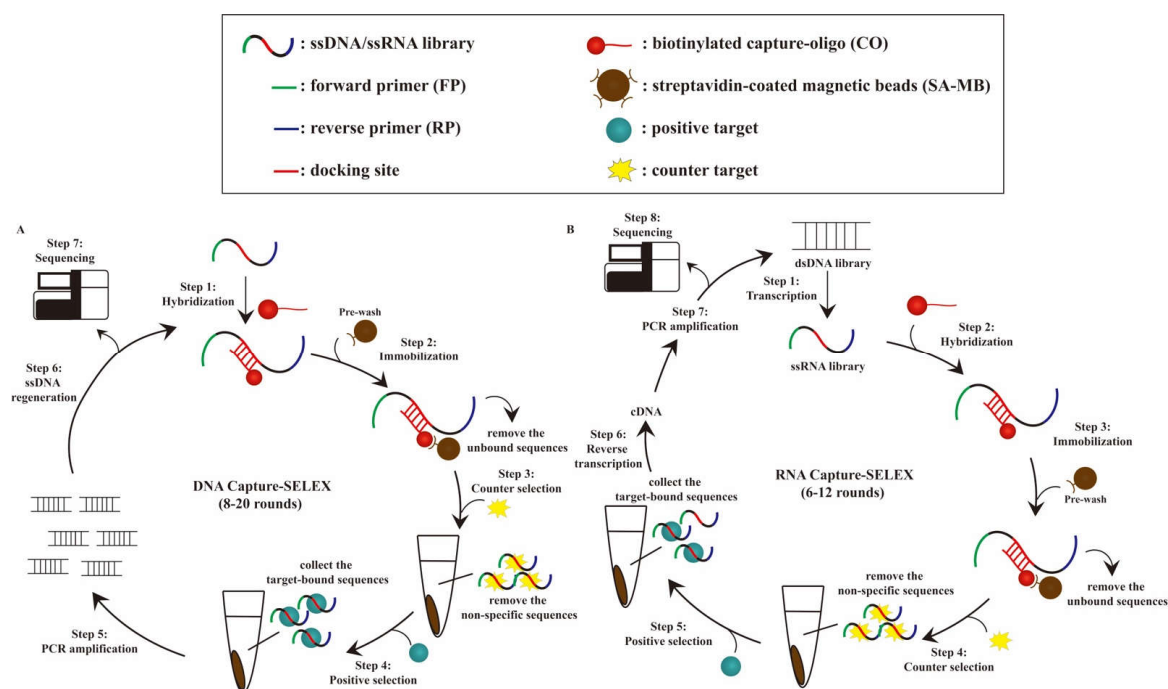


Figure 1. The experimental flowchart of DNA Capture-SELEX and RNA Capture-SELEX. **(A)** DNA Capture-SELEX. Each DNA Capture-SELEX selection round consists of 7 main steps: (1) The designed ssDNA library template is hybridized with biotinylated capture-oligonucleotide. (2) The hybridized product is immobilized on the washed streptavidin-coated magnetic beads. (3–4) Target-bound sequence elution: counter selection is followed by positive selection. (5) PCR amplification was performed on the eluted ssDNA to obtain the amplified dsDNA pool, (6) and regenerate ssDNA for the next DNA Capture-SELEX round (either gel purification or magnetic bead-based method). (7) After DNA Capture-SELEX, aptamer sequences were identified through sequencing. **(B)** RNA Capture-SELEX. The principles and procedures are similar to **(A)**, except that RNA Capture-SELEX consists of additional transcription (step 1) to convert DNA to RNA and reverse transcription (step 6) to convert RNA to DNA steps.

2. Principle and General Procedure of Capture-SELEX for Aptamer Selection

2.1. Overview of DNA and RNA Capture-SELEX

The classical procedure of the DNA Capture-SELEX selection method involves hybridization, immobilization, target-bound sequence elution, polymerase chain reaction (PCR) amplification, regeneration of single-stranded DNA (ssDNA), and sequencing (Figure 1A). Briefly, in the first step, a random ssDNA library is designed with a docking site that is complementary to the biotinylated capture oligonucleotides, and these ssDNAs are hybridized with capture-oligonucleotides to form biotinylated hybridized library via Watson-Crick base pairing. Next, the biotinylated library is immobilized onto SA-MBs, which function as solid support, and the loaded SA-MBs are then washed several times to remove the residual and non-specific sequences using a magnetic rack and generate a washed biotinylated library on the MBs (which comprise superparamagnetic iron oxide). Subsequently, a magnetic rack also used to discard supernatant (unbound or non-specific sequences), after which the counter-selection process is performed, wherein a counter target with a similar chemical structure and concentration as the positive targets, enhances the binding affinity and specificity of aptamers towards it positive small-molecule target [42]. Counter selection can be performed either in the last few rounds [39,43] or between the selected rounds [44,45] of Capture-SELEX, and the concentration of the counter target should be the same as the positive target in step 3 (Figure 1A). The negative selection is followed by positive selection. Next, an elution is performed; if the binding affinity between the target and aptamer is higher than that between the aptamer and the capture

oligonucleotide, the target-bound aptamer candidates are eluted. As the library sequences interact with the positive targets, only sequences with conformational changes due to the interaction can be eluted from the MBs [46].

In this review, we summarize two main strategies used to regenerate ssDNA from amplified dsDNA in step 6 (Figure 1A): the gel purification method [21,23,47] and the MB-based method [24]. A primer is designed and modified in order to identify the sense strand in the denaturing polyacrylamide gel, such as a reverse primer with poly-dA₂₀ extension or a forward primer labeled with either fluorescein or the cyanine dye Cy3. The gel purification method involves denaturing polyacrylamide gel electrophoresis (PAGE), followed by extraction and purification. The MB-based method begins with PCR products with biotinylated reverse primers being incubated to facilitate their deposition onto MBs. The supernatant is then removed, and the non-biotinylated forward strands of dsDNA PCR products are released from the MBs by treatment with sodium hydroxide and then neutralized by treatment with an appropriate amount of tris(hydroxymethyl)aminomethane hydrochloride or hydrochloric acid. The regenerated ssDNA in each round is collected for the next round of selection and then prepared for sequencing after several rounds of selection. Currently, Capture-SELEX is mostly applied for the selection of DNA aptamers rather than RNA aptamers. RNA Capture-SELEX adopts the same selection strategies as DNA Capture-SELEX, except for including two more steps: transcription and reverse transcription (Figure 1). In addition, more rounds need to be performed in DNA Capture-SELEX (8–20 rounds) than in RNA DNA Capture-SELEX (6–12 rounds) to enrich the target-bound pool sufficiently.

2.2. Sanger and Next-Generation Sequencing and Analysis

Sequencing is a crucial step performed after the SELEX-based selection of aptamer candidates and before aptamer–target characterization. Here, we review two of the main methods used for sequencing aptamers, those being Sanger sequencing and next-generation sequencing (NGS). Sanger sequencing is a DNA sequencing technology based on the chain termination method invented by Frederick Sanger and his colleagues [48] in 1997. The main workflow involves blocking the polymerase-mediated elongation of DNA through the incorporation of fluorophore-labeled dideoxynucleotides (dideoxyadenosine triphosphate, dideoxyguanine triphosphate, and dideoxythymine triphosphate) at the 3' ends of DNA sequences, resulting in various lengths of DNA fragments for size separation and fluorescent-based detection. This method has the advantages of high precision, high efficiency, and low radioactivity, and the disadvantages of being expensive and having low-quality primer binding in the first 15 to 40 base pairs [49]. Subsequently, high-throughput second- and third-generation sequencing were invented and superseded Sanger sequencing [50]. In 1998, Balasubramanian and Klenerman co-invented Solexa sequencing [51], also known as NGS. This method differs from Sanger sequencing mainly in its mode of chain termination: modified deoxynucleoside triphosphates (dNTPs) with a reversible terminator are used to terminate polymerization and are then removed to allow incorporation of the next modified dNTP [52]. NGS offers some advantages over Sanger sequencing, including enabling massively parallel sequencing in a short period and having a lower cost per base pair.

In order to analyze sequencing data, *in silico* technique towards SELEX facilitate the aptamer selection [53–55]. The initial step is primary sequence analysis using some bioinformatic tools, such as ClustalW [56] and Clustal Omega (<https://www.ebi.ac.uk/Tools/msa/clustalo/> (accessed on 12 October 2022)) [57]. Multiple sequence alignment is performed to divide sequences into families or clusters. The conserved regions of the sequences are analyzed using Gblocks software. Furthermore, Multiple Expectation maximizations for Motif Elicitation (<https://meme-suite.org/meme/tools/meme> (accessed on 12 October 2022)) [58] is used to identify the sequence motif, which provides the basis for downstream analysis. Aptamers can form diverse secondary structures, such as stem-loop, triplex, G-quadruplex, and pseudoknot structures; thus, enriched sequences can also be selected based on secondary structure and Gibbs free energies (ΔG) prediction. Several nu-

cleic acid structure-prediction Web servers are available and are often used to computationally predict secondary structures and Gibbs free energies (ΔG) of aptamer sequences. These include MFOLD (<http://www.unafold.org/mfold/applications/dna-folding-form.php> (accessed on 12 October 2022)) [59], KineFold (<http://kinefold.curie.fr/> (accessed on 12 October 2022)) [60], and RNAstructure (<https://rna.urmc.rochester.edu/RNAstructure.html> (accessed on 12 October 2022)) [61]. The predicted secondary structures were then converted into unique three-dimensional (3D) structures using online web servers. These include fragment-based methods: RNAComposer (<https://rnacomposer.cs.put.poznan.pl/> (accessed on 12 October 2022)), 3dRNA (<http://biophy.hust.edu.cn/3dRNA> (accessed on 12 October 2022)), and Vfold 3D (<http://rna.physics.missouri.edu/vfold3D/> (accessed on 12 October 2022)); and energy-based method: simRNA (<https://genesilico.pl/SimRNAweb> (accessed on 12 October 2022)) [62]. Molecular docking tools include AutoDock, AutoDock Vina, and DOCK, which were used to predict the predominant binding modes and regions of the target molecule based on the generated binding scores for specific sequences [63–65]. After a few prediction steps, the aptamer candidates are shortlisted and subjected to binding tests and characterization.

3. Small-Molecule–Aptamer Interaction and Characterization

The secondary structures of aptamers often organize into complex three-dimensional structures to maintain global stability and form functional conformations. Therefore, a stable aptamer can strongly bind to small molecules and shape the aptamers–target complex via weak noncovalent interaction forces, including hydrogen bonding, π - π stacking, van der Waals forces, hydrophobic, and electrostatic interactions. The aptamer–target interactions may either depend on the availability of narrow binding pockets in the three-folded structures of aptamers or the chemical characteristics of targets and the aptamer candidate or the length of the oligonucleotides, for example, removing excess flanking nucleotides outside the binding site (truncated aptamer), which is also a strategy to improve binding affinity and specificity [66,67]. In order to assess the binding strength and specificity of the interaction between an aptamer and its target, binding assays are used to determine the dissociation constant (K_d) (Table 1), i.e., the binding affinity between an aptamer and its cognate target (and between an aptamer and its non-cognate targets), where the lower the K_d value, the stronger the interaction. Several factors may influence the K_d value, such as temperature, pH value, ionic concentrations, and hydrophobicity of the solution [66]. Below, we discuss the six standard assays used for characterizing the interactions between small-molecule contaminants and aptamers generated using DNA/RNA Capture-SELEX (Figure 2). In contrast with traditional methods, such as HPLC and LC-MS, these assays are highly sensitive, non-toxic, and inexpensive.

Table 1. A list of small molecule contaminant-specific aptamers developed by Capture-SELEX method as of to date.

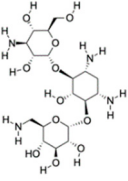
| Name | Class | Aptamer Sequence (5'–3') | nt | Dissociation Constant (K_d) | Ref. |
|--|---------------------------|--|----|---------------------------------|------|
| Kanamycin A CAS no.: 59-01-8  | Aminoglycoside antibiotic | ATACCAGCTTATTCAATTAGCCCGGTATTGA GGTCGATCTCTTATCCTATGGCTT GTCCCCCAT GGCTCGGTTATATCCAGATAGTAAGTGCAATCT | 97 | 3.9 μ M | [22] |

Table 1. Cont.

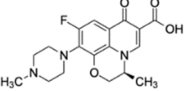
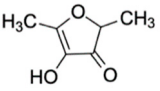
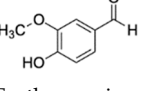
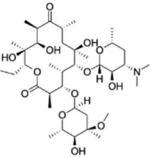
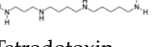
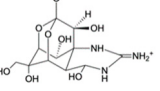
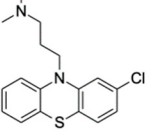
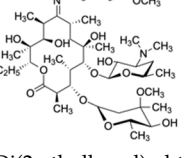
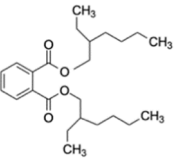
| Name | Class | Aptamer Sequence (5'-3') | nt | Dissociation Constant (K_d) | Ref. |
|---|----------------|--|----|---------------------------------|------|
| Ofloxacin CAS no.: 82419-36-1  | Antibiotic | ATACCAGCTTATTCAATTGCAGGGTAT CTGAGGCTTGATCTACTAAATGTCGT GGGGCATTGCTATTGGCGTTGATACGTA CAATCGTAATCAGTTAG | 98 | 0.11 ± 0.06 nM | [39] |
| Furaneol CAS no.: 3658-77-3  | Aroma compound | CGACCAGCTCATTCTCACCACGA GAAAGGAGCTCGATGAAGTGCAGC CGGATTTCGACCCTATGCGAGTAGGTG GTGGATCCGAGCTCACCAGTC | 96 | 1.1 ± 0.4 μ M | [68] |
| Vanillin CAS no.: 121-33-5  | Flavoring | CGACCAGCTCATTCTCAGGAGAAA CATGGAGTCTCGATGATGTAGGAGCGG CGGAACGTAGGAAGAGA GGATGACGGAGGATCCGAGCTCACCAGTC | 98 | 0.9 ± 0.3 μ M | [23] |
| Erythromycin CAS no.: 114-07-8  | Antibiotic | AGGAATTCACGTCTCACTGGATTCACGCAC GCCAAGGACTGCCTTAAGGTTAGA TAGCCCCATGCAGTGAGTCAGGATATCG | 83 | 20 ± 9 nM | [24] |
| Spermine CAS no.: 71-44-3  | Biogenic amine | TATGAACGATTTACTCGTACAGA CGACACTTATCATTTCG | 40 | 9.648 ± 0.896 nM | [44] |
| Tetrodotoxin CAS no.: 4368-28-9  | Toxin | ATACCAGCTTATTCAATTTAATGCGGG GTGAGGCTCAATCAAGGAAAGATATAAGTAA GCAAAAAGGTCAAACAAGGGCGA GATAGTAAAGTGAATCT | 98 | 7 ± 1 nM | [43] |
| Chlorpromazine CAS no.: 50-53-3  | Phenothiazine | TCGGAGGGAAGTGCACCCATTCTTGAAACAG GAGCTCCTGAACCGCCCACACGC | 55 | 69.8 ± 9.81 nM | [69] |
| Roxithromycin CAS no.: 80214-83-1  | Antibiotic | ATTGGCACTCCACGCATAGGCACACCCAC CGGCTAGCCACACCATGCTGTGTTGC CCACCTATGCGTGCTACCGTGAA | 80 | 0.46 ± 0.08 μ M | [70] |
| Di(2-ethylhexyl) phthalate (DEHP) CAS no.: 117-81-7  | Plasticizer | ACGCATAGGGTGCGACCACAT ACGCCCCATGTATGTCCTTGGTT GTGCCCTATGCGT | 58 | 2.26 ± 0.06 nM | [71] |

Table 1. Cont.

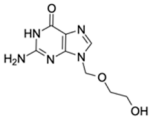
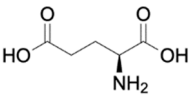
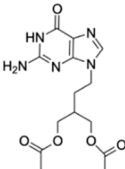
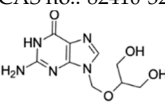
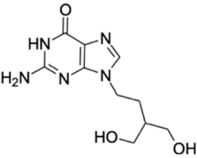
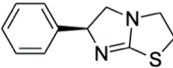
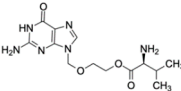
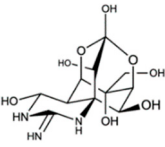
| Name | Class | Aptamer Sequence (5'-3') | nt | Dissociation Constant (K_d) | Ref. |
|--|-----------------------------|--|----|---------------------------------|------|
| Acyclovir (ACV) CAS no.: 59277-89-3  | Aminoglycoside Antibiotics | TGAGCCCAAGCCCTGGTATGTGAAAACATACT AGACGTGGCTATGTATTTTTAAATCAA TGCCAGGTCTACTTTGGGATC | 80 | 32.67 ± 4.127 nM | [72] |
| Glutamate CAS no.: 56-86-0  | Excitatory neurotransmitter | GCATCAGTCCACTCGTGAGGTCGACTGA TGAGGCTCGATCAGGAGCGCCGCTCG ATCGCACTTTCACAGGATAGTAGTTG GTAGCGACCTCTGCTAGA | 98 | 12 ± 6 μ M | [73] |
| Famciclovir (FCV) CAS no.: 104227-87-4  | Aminoglycoside Antibiotics | TGAGCCCAAGCCCTGGTATGTGAAAACA TACTAGACGTGGCTATGTATTTTTAAAT CAATGGCAGGTCTACTTTGGGATC | 80 | 47.35 ± 10.42 nM | [72] |
| Ganciclovir (GCV) CAS no.: 82410-32-0  | Aminoglycoside Antibiotics | TGAGCCCAAGCCCTGGTATGTGAAA ACATACTAGACGTGGCTATGTATTTTTAA ATCAATGGCAGGTCTACTTTGGGATC | 80 | 47.91 ± 13.47 nM | [72] |
| Penciclovir (PCV) CAS no.: 39809-25-1  | Aminoglycoside Antibiotics | TGAGCCCAAGCCCTGGTATGTGAAA CATACTAGACGTGGCTATGTATTTTT AAATCAATGGCAGGTCTACTTTGGGATC | 80 | 33.29 ± 5.851 nM | [72] |
| Levamisole (LEV) CAS no.: 14769-73-4  | Veterinary drug | AATCAAACGCTAAGGTCAAGGGAGAG TGCACCCATTCTTTGGGCCCCGGGC CAGCCCCGACACGCCCGGAAG CTTGGTACCCGTATCGT | 90 | 66.15 ± 11.86 nM | [74] |
| Valaciclovir (VACV) CAS no.: 124832-26-4  | Aminoglycoside Antibiotics | TGAGCCCAAGCCCTGGTATGTGAAA ACATACTAGACGTGGCTATGTATTTTT TAAATCAATGGCAGGTCTACTTTGGGATC | 80 | 44.26 ± 6.744 nM | [72] |
| Tetrodotoxin CAS no.: 4368-28-9  | Toxin | ATACCAGCTTATTCAATTTAATGCGGGGTGAGG CTCAATCAAGGAAAGATATAAGTAAAGCAAAAAG GTCAAACAAGGGCGAGATAGTAAAGTCAATCT | 98 | 7 ± 1 nM | [43] |

Table 1. Cont.

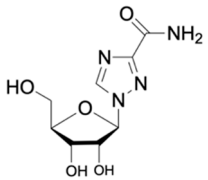
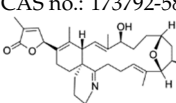
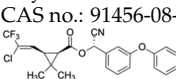
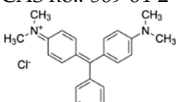
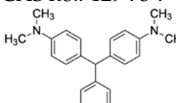
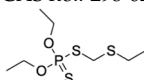
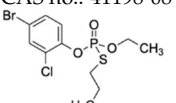
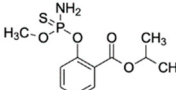
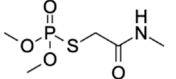
| Name | Class | Aptamer Sequence (5'-3') | nt | Dissociation Constant (K_d) | Ref. |
|--|------------------------------------|---|--------------|---|------------------|
| Ribavirin CAS no.: 36791-04-5  | Antiviral agent | AAAGTAATGCCCGGTAGTTATTCAAAGATGA GTAGGAAAAGA | 42 | 61.19 ± 21.48 nM | [45] |
| Gymnodimine-A CAS no.: 173792-58-0  | Toxin | GCGACCGAAGTGAGGCTCGATCCAAGGTG GACGGGAGGTTGGATTGTGCGTG | 52 | 34.5 ± 1.72 nM | [75] |
| λ -cyhalothrin CAS no.: 91456-08-6  | Pesticide | AGGGGAAGCACGGGCGGGCG | 20 | 10.27 ± 1.33 nM | [76] |
| Malachite green (MG) CAS no.: 569-64-2  | Veterinary drug | (1) CGCAGCGCGGCAGACAGTCAGGCTC AGCACGTGGCA (2) CACTCCACGCATAGGGACGCGAATTGCG GACCTATGTGTGGTGTG | 36 45 | 102.46 μ M 2.3 ± 0.2 μ M | [77] [78] |
| Leucomalachite green (LMG) CAS no.: 129-73-7  | Antimicrobial | CACTCCACGCATAGGGACGCGAATTGCGGA CCTATGTGTGGTGTG | 45 | 8.2 ± 1.2 μ M | [78] |
| Phorate CAS no.: 298-02-2  | Organothiophosphate insecticide | AAGCTTGCTTTATAGCCTGCAGCGAT TCTTGATCGGAAAAGGCTGAGAGCTACGC | 55 | 1.11 μ M | [79] |
| Profenofos CAS no.: 41198-08-7  | Organothiophosphate insecticide | AAGCTTGCTTTATAGCCTGCAGCGATT TTGATCGGAAAAGGCTGAGAGCTACGC | 55 | 1 μ M | [79] |
| Isocarbophos CAS no.: 24353-61-5  | Organothiophosphate insecticide | AAGCTTGCTTTATAGCCTGCAGCGATTCTTGATCG GAAAAGGCTGAGAGCTACGC | 55 | 0.83 μ M | [79] |
| Omethoate CAS no.: 1113-02-6  | Organothiophosphate insecticide | AAGCTTTTTGACTGACTGCAGCGATT TTGATCGCCACGGTCTGGAAAAGAG | 54 | 2 μ M | [79] |

Table 1. Cont.

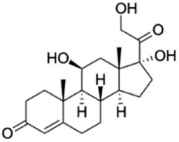
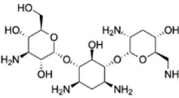
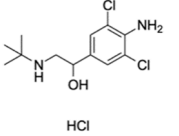
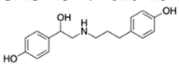
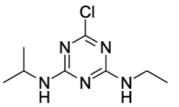
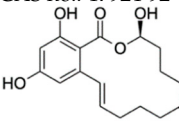
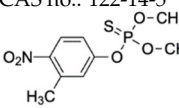
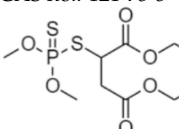
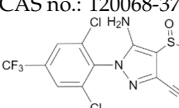
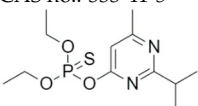
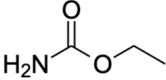
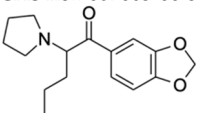
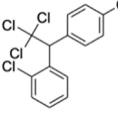
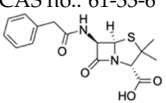
| Name | Class | Aptamer Sequence (5'-3') | nt | Dissociation Constant (K_d) | Ref. |
|---|------------------------------|--|----|---------------------------------|------|
| Cortisol CAS no.: 50-23-7  | Steroid hormone | GGAATGGATCCACATCCATGGATGGGCAATG CGGGTGGAGAATGGTTGCCGCA CTTCGGCTTC ACTGCAGACTTGACGAAGCTT | 85 | 6.9 ± 2.8 nM | [80] |
| Tobramycin CAS no.: 32986-56-4  | Aminoglycoside antibiotic | CCATGATTCAACTTACTGGTCTGTCT TGGCTAGTCGTGTGCATTCCCCTAAGGG | 57 | 200 nM | [47] |
| Clenbuterol hydrochloride (CLB) CAS no.: 21898-19-1  | beta-adrenergic agonist | AGCAGCACAGAGGTCAGATGTCATCTGAAG TGAATGAAGGTAACATTATTCATTAA CACCTATGCGTGCTACCGTGAA | 80 | 76.61 ± 12.7 nM | [81] |
| Ractopamine CAS no.: 97825-25-7  | Veterinary drug | AGCAGCACAGAGGTCAGATGGTCTCTAC TAAAAGTTTTGATCATACCGTTCACATAATG ACCTATGCGTGCTACCGTGAA | 80 | 54.22 ± 8.02 nM | [82] |
| Atrazine CAS no.: 1912-24-9  | Herbicide | TGTACCGTCTGAGCGATTCTACTTTATTTCG GGAAGGGTATCAGCGGGTTCAACAA GCCAGTCAGTCAGTGTTAAGGAGTGC | 83 | 3.7 nM | [83] |
| Zearalenone CAS no.: 17924-92-4  | Mycotoxin | ATACCAGCTTATTCAATTCTACCAGCTTT GAGGCTCGATCCAGCTTATTCAATTATA CCAGCTTATTCAATTATACCAGCACAATC GTAATCAGTTAG | 98 | 15.2 ± 3.4 nM | [84] |
| Fenitrothion CAS no.: 122-14-5  | Phosphorothioate insecticide | CTCTCGGGACGACGGGCCGAGTAGTCTCCAC GATTGATCGGAAGTCGTCCC | 51 | 33.57 nM | [85] |
| Malathion CAS no.: 121-75-5  | Organophosphate insecticide | GGGATACAGGTAGTATGGCATGTGCTAGCG GTTGCA | 36 | 22.56 nM | [86] |
| Fipronil CAS no.: 120068-37-3  | Insecticide | ACGACAGATAGTGTGTACATGAAGGGTCGT | 30 | 15 nM | [87] |

Table 1. Cont.

| Name | Class | Aptamer Sequence (5'-3') | nt | Dissociation Constant (K_d) | Ref. |
|--|-----------------------------|---|----|---------------------------------|------|
| Diazinon CAS no.: 333-41-5  | Organophosphate insecticide | TTCCGATCAATCGTGGAGACTACTCGGCC | 30 | $4.571 \pm 0.714 \mu\text{M}$ | [88] |
| Ethyl carbamate (EC) CAS no.: 51-79-6  | Organic compound | GGGGGCACGGGAGGT | 15 | $17.97 \pm 0.98 \text{ nM}$ | [89] |
| 3,4-methylenedioxypropyl- alerone (MDPV) CAS no.: 687603-66-3  | Synthetic cathinone | CTTACGACTCAGGCATTTGCCGGGTAAC GAAGTACTGTCTGTAAG | 46 | $6.1 \pm 0.2 \mu\text{M}$ | [90] |
| Dichlorodiphenyltrichloroethane (o,p'-DDT) CAS no.: 789-02-6  | Insecticide | TCCAGCACTCCACGCATAACGAATTGTGC TCAATGCGCCCCCTGCAGTGAATGTGGAATT TGTTATGCGTGCGACGGTGAA | 80 | $412.3 \pm 124.6 \text{ nM}$ | [91] |
| Penicillin G CAS no.: 61-33-6  | β -lactam antibiotic | GGGAGGACGAAGCGGAACGAGATGTAGAT GAGGCTCGATCCGAATGCGTGACGTCTATCGGA ATACTCGTTTTTACGCCTCAGAAGACACGCCGACA | 98 | – | [21] |

3.1. SYBR Green I (SGI) Assay

The binding affinity of Capture-SELEX-generated aptamers for small molecules can be identified by a novel label-free fluorescence SGI assay [24,68,70,73,83]. SGI is a fluorescent nucleic-acid-intercalating dye that was introduced in the 1990s and is widely applied in real-time PCR [92–94], fluorescent gel imaging [95,96], and flow cytometry [97,98]. It intercalates into the minor groove of DNA base pairs or adenine–thymine-rich stem-loop sites to form a fluorescent complex with DNA [99]. The fluorescence intensity of SGI–DNA complexes is measured in the range of 505 to 650 nm, with an excitation wavelength of 495 nm and an emission wavelength of 525 nm, using a spectrophotometer or a microplate reader; thus, an SGI assay identifies the binding affinity of aptamers for small-molecule targets by detecting the change in the fluorescent signal induced by the dissociation of SGI from the aptamers upon their binding with these small-molecule targets, and therefore the fluorescence intensity decreases (Figure 2A). The fluorescence intensity will be recovered as the concentration of the aptamers' small-molecule targets increases.

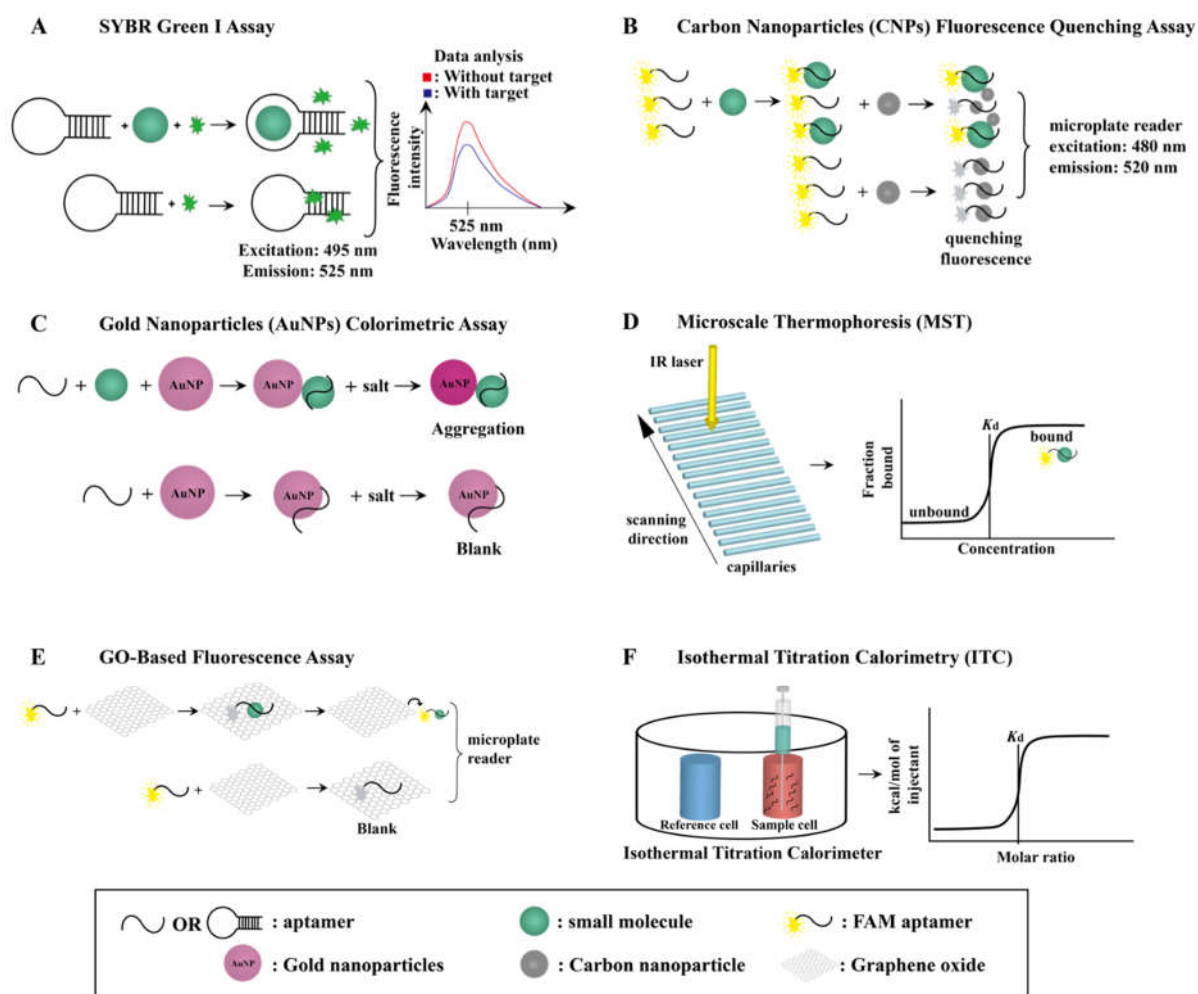


Figure 2. A schematic illustration of six commonly used methods for detecting interactions between small molecule and aptamer. (A) SYBR green I (SGI) assay. (B) Carbon nanoparticles (CNPs) fluorescence quenching assay. (C) Gold nanoparticles (AuNPs) colorimetric assay. (D) Microscale thermophoresis (MST) assay. (E) Graphene oxide (GO)-based fluorescent assay. (F) Isothermal titration calorimetry (ITC) assay.

3.2. Carbon Nanoparticle (CNP) Fluorescence Quenching Assay

CNPs can be readily synthesized [45] in research laboratories, have low toxicity, and are biocompatible [100]. Due to the strong fluorescence-quenching ability of CNPs' sp^2 - and π -rich structures, they are useful for characterizing the binding affinity of aptamers for small molecules. This means that when an aptamer is adsorbed onto the surface of CNPs, π - π stacking interactions that form between the nucleobases and nucleosides of the aptamer and the CNPs result in fluorescence quenching. Therefore, in the absence of aptamers' small-molecule targets, aptamers are bound to CNPs, resulting in fluorescence quenching, whereas in the presence of aptamers' small-molecule targets, aptamers are bound to these targets rather than CNPs, and thus fluorescence is not quenched (Figure 2B) [101].

3.3. Gold Nanoparticle (AuNP) Colorimetric Assay

The AuNP colorimetric assay is widely used for characterizing the binding affinity of an aptamer for its target [24,45,70,71,76,80,83,84]. It is a label-free assay as AuNPs allow the identification of a target reaction based on colorimetric signals. AuNPs can be synthesized by reducing chloroauric acid with citric acid and ascorbic acid (the Turkevich method) [102] or with sodium citrate [103]. The Turkevich method affords AuNPs coated with negatively charged citrate ions, and thus the AuNPs are treated with sodium chloride to neutralize

their surface charge and thereby induce their aggregation (Figure 2C) [104]. Owing to the electrostatic screening effect, the surface plasma resonance absorption peak of AuNPs undergoes a red shift from 520 nm to 650 nm, which is measured using a microplate reader and reflects the binding affinity of aptamers to their small-molecule targets. In the absence of their small-molecule target, aptamers are adsorbed onto the surface of AuNPs, increasing their colloidal stability of AuNPs and reducing their salt-induced aggregation [105]. However, in the presence of their small-molecule targets, aptamers binds to their targets rather than AuNPs, which decreases the colloidal stability of AuNPs and thereby increases their salt-induced aggregation. This results in a solution containing AuNPs, aptamers, and their small-molecule targets changing color from red to pink to purple or even to blue or gray [70].

3.4. Microscale Thermophoresis (MST) Assay

The MST assay is a powerful tool for testing the binding affinity of aptamers for their small-molecule targets as it only requires a small amount of sample (up to 4 μ L), involves a simple preparation process, and rapidly provides accurate results (within 15 min) [75,76,80]. It is a fluorophore-labeled and immobilization-free assay that is carried out using a Monolith NT.115 instrument. As shown in Figure 2D, the capillary tray of this instrument can accommodate up to 16 thin glass capillaries for operation. An infrared laser heats a specific capillaries area, creating a microscopic temperature gradient on them. Thus, when an aptamer binds to its small-molecule target, there is a significant change in fluorescence intensity due to thermophoresis. An MST binding curve (dose-response curve) is plotted using Affinity Analysis Software to represent specific binding that is specific to its small-molecule target, which automatically calculates the K_d of an aptamer for its small-molecule target.

3.5. GO-Based Fluorescent Assay

GO can be synthesized from graphite via the Hummers and Offeman method [106], which uses potassium permanganate (as the oxidizing agent) and sodium nitrate in a solution of sulfuric acid [107]. GO has an sp^2 structure and numerous oxygen-containing functional groups [108], such as carbonyl groups, hydroxyl groups, and carboxylic acid groups, and thus can strongly quench fluorescence. This quenching occurs when a 5'-fluorescein-labeled aptamer is adsorbed onto the surface of GO through π - π stacking interactions and hydrogen bonding (Figure 2E). When 5'-fluorescein labeled aptamer is absorbed onto GO, GO-mediated fluorescence quenching occurs. The fluorescence intensity will be recovered when the labeled aptamer is desorbed from the surface of GO in the presence of small-molecule target. The fluorescence intensity change are measured using a microplate reader, and eventually the K_d value of the aptamer for its small-molecule target is calculated [72,77,109].

3.6. Isothermal Titration Calorimetry (ITC) Assay

The ITC assay is a label-free and immobilization-free assay for measuring the binding affinity of an aptamer for its small-molecule target [44,83] in an instrument comprising a reference cell and a sample cell (Figure 2F). The reference cell is filled with a buffer and water (without the aptamer or its small-molecule target), while the sample cell is filled with the buffer and the aptamer and is titrated via syringe with up to 20 volumes of the aptamer's small-molecule target [77]. The temperature in the two cell units is maintained at a constant value, and when the small molecule is titrated against the aptamer in the sample cell, an exothermic binding reaction occurs. The feedback system of the ITC instrument then reduces the power supply to the sample cell to prevent an increase in temperature, leading to a difference in the amount of energy supplied to the reference cell and the sample cell. Therefore, during this titration, the power supply to the sample cell continuously decreases until the small-molecule-aptamer binding has been completed. The binding affinity of the aptamer can then be determined from the energy curve generated [110].

The ITC instrument measures the exothermic reaction (heat released) and endothermic reaction (heat absorbed) when the molecules interact. The peak goes downward when the exothermic reaction occurs, whereas an upward peak is measured when an endothermic reaction occurs. The downward peak between the interaction of aptamer and small-molecule target are measured from the ITC instrument using software such as MicroCal ITC200 and MicroCal PEAQ-ITC.

4. Development of Aptamer-Based Biosensors

To date, Capture-SELEX has been used for screening and generating a series of aptamers against small-molecule contaminants (Table 1). As aptasensors can be used for low-cost, rapid, and real-time detection of small-molecule contaminants, they have increasingly supplanted conventional antibody-based biosensors. Fluorescent aptasensors are the most popular (Table 2), and their working principle is similar to that of fluorescent-based characterization methods. Therefore, two other types of aptasensor are discussed here (Figure 3).

Table 2. Representative biosensors using aptamers against small molecule contaminants that are generated from Capture-SELEX.

| Types | Aptamer Targets | Limit of Detection (LOD) | Detection Range | Ref. |
|---|-----------------------------------|--------------------------|---------------------|----------------------|
| Ion-sensitive field-effect transistor (ISFET) | Vanillin | 0.155 μ M | 0.155–1.0 μ M | [23] |
| | Furaneol | – | 0.1–10 μ M | [68] |
| Electrochemical impedance spectroscopy (EIS) | Penicillin G | 0.00051 μ M | 1.2 nM–2.99 μ M | [21] |
| | Di(2-ethylhexyl) phthalate (DEHP) | 0.264 pM | – | [71] |
| | Glutamate | 0.0013 pM | 0.01 pM–1 nM | [73] |
| | Spermine | 0.052 nM | 0.1–20 nM | [44] |
| | Tyramine (TYR) | 2.48 nM | 3.64–728.97 nM | [109] |
| | β -phenethylamine | 3.22 nM | 4.13–825.22 nM | [109] |
| | Acyclovir | 2.13 nM | 8.88–444.03 nM | [72] |
| | Famciclovir | 1.74 nM | 6.22–311.2 nM | [72] |
| | Ganciclovir | 2.08 nM | 7.84–391.80 nM | [72] |
| | Penciclovir | 1.97 nM | 7.9–394.85 nM | [72] |
| | Valaciclovir | 1.17 nM | 6.17–308.32 nM | [72] |
| | Ribavirin | 2.74 nM | 4.09–204.75 nM | [45] |
| | Fluorescent | Malachite Green | 5.84 nM | 4.69 nM–2.35 μ M |
| Cadmium ions (Cd(II)) | | 40 nM | 0–1000 nM | [111] |
| Clenbuterol hydrochloride (CLB) | | 0.22 nM | 0.32–159.44 nM | [81] |
| Ractopamine | | 0.13 nM | 0.33–331.79 nM | [82] |
| Chlorpromazine | | 0.67 nM | 1–100 nM | [69] |
| Fenitrothion | | 14 nM | 0–80 nM | [85] |
| Malathion | | 6.08 nM | – | [86] |
| Fipronil | | 3.4 nM | 0–70 nM | [87] |
| Diazinon | | 148 nM | 0.1–25 μ M | [88] |
| Erythromycin | | 3 pM | 1 pM–10 nM | [24] |
| Ethyl carbamate | | 0.024 μ M | 0.11–0.67 μ M | [89] |
| Roxithromycin | | 0.077 μ M | 0–4.44 μ M | [70] |
| Colorimetric | | λ -cyhalothrin | 41 nM | 0.22–1.11 μ M |
| | Zearalenone | 12.5 nM | 12.5–402.1 nM | [84] |
| Biolayer interferometry (BLI) | Levamisole | 1.12 nM | 1–200 nM | [74] |
| | Gymnodimine-A | 6.21 nM | 55–1400 nM | [75] |

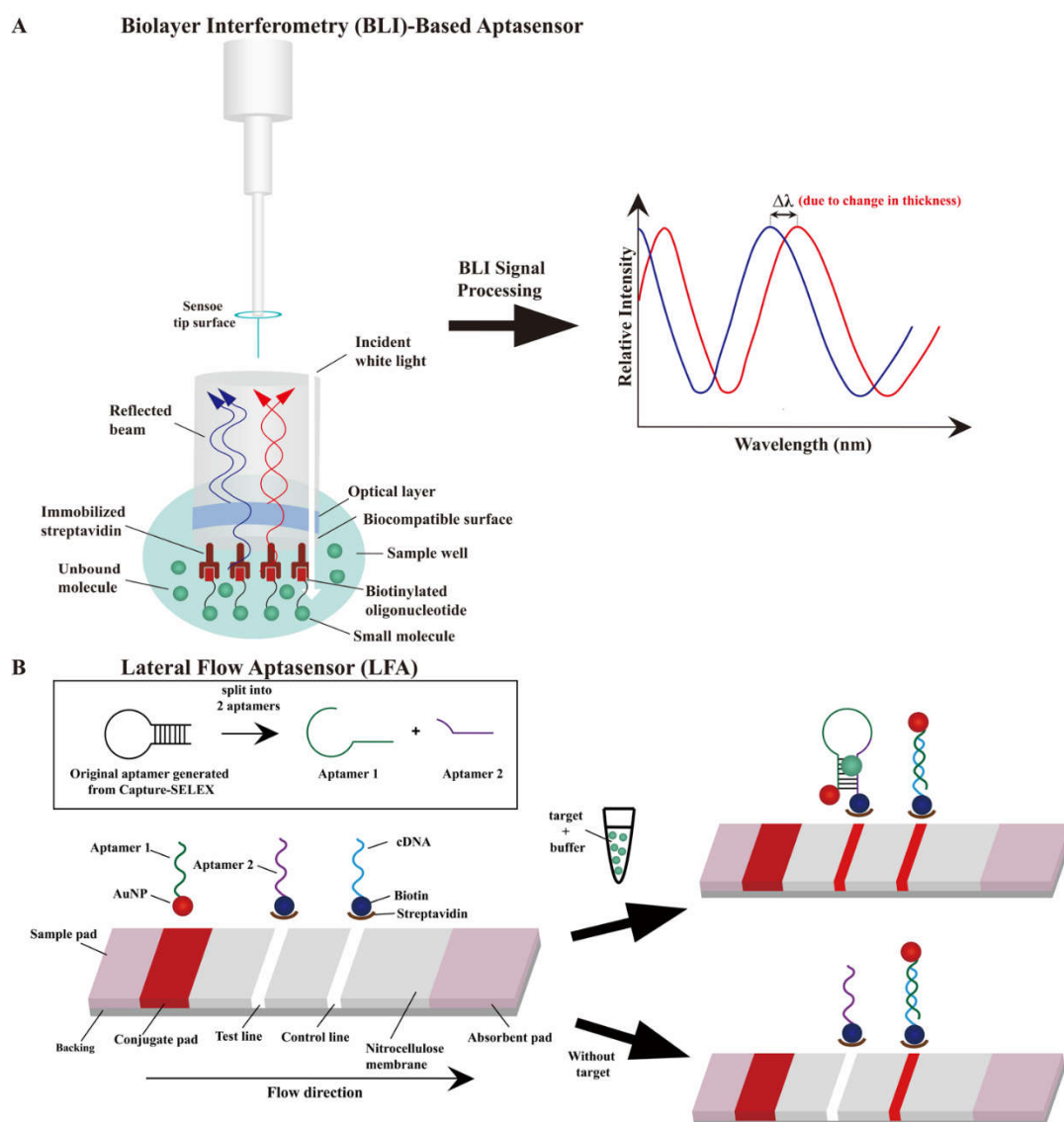


Figure 3. The schematic illustration of aptasensors for the detection of small molecules using novel aptamer generated from Capture-SELEX. (A) Biolayer interferometry (BLI)-based aptasensor. (B) A lateral flow aptasensor (LFA) is generally constructed by 4 sections: sample pad, conjugate pad, nitrocellulose membrane with test line and control line, and absorbent pad. The sample flow from left to right laterally (left). When the target is loaded onto the sample pad, positive result (red band for both control and test line) is observed after 15 min (right).

4.1. Biolayer Interferometry (BLI)-Based Aptasensor

Optical-fiber-based BLI biosensors have been developed for real-time, sensitive, and rapid measurement [112] of interactions between biomolecules, including DNA–protein [113,114], antibody–antigen [115], and DNA–small-molecule-contaminant interactions [116,117]. The sensor tip of an optical fiber consists of two reflective surfaces: a streptavidin-coated biocompatible surface, which is immersed in the sample solution, and an optical layer, which functions as an internal surface (Figure 3A). The biocompatible surface is functionalized to immobilize a biotinylated aptamer and minimize non-specific binding. Inside the sensor, these two surfaces generate an interference pattern by reflecting incident white light. When an aptamer binds to its small-molecule target, a spectral redshift ($\Delta\lambda$) occurs as the bound compound immobilizes on the tip surface and the surface thickness increases. The false-positive results from this sensor can be minimized as the

non-specific and unbound molecules can be differentiated from the molecules with high binding affinity, resulting in high detection accuracy [116].

4.2. Lateral Flow Aptasensors (LFAs)

LFAs have been developed as portable detection devices with cost-effective, rapid (≤ 15 min), and easy operation and broad applications, such as in the detection of pregnancy, severe acute respiratory syndrome coronavirus 2 [118,119], and infectious diseases [120]. Owing to the drawbacks of antibodies, LFAs are gradually replacing antibody-based lateral flow biosensors, although the latter remains predominantly used. In addition, LFAs have been used to detect antibody-inaccessible small-molecule contaminants [24,89,121]. Figure 3B depicts the LFA concept [121–123], in which AuNPs are typically used for colorimetric identification of the test line and control line on the strip [124]. The high affinity aptamer generated from Capture-SELEX against the specific small-molecule target that splits into two fragmented aptamers (aptamer 1 and 2; Figure 3B) [123]. A sample solution (a solution of an aptamer's small-molecule target in buffer) is loaded onto the sample pad and flows through the conjugate pad (containing AuNP–aptamer 1 conjugates) by capillary action. When aptamer–small-molecule-target binding occurs, two fragmented aptamers could rejoin the three-dimensional structure without affecting the binding affinity, and thus a red band appears in the test line. A complementary DNA (cDNA) is designed to hybridize with aptamer 1 in the control line and generate a visual signal, which is used to verify whether the aptasensor is working properly based on the appearance of red band in both presence or absence of the aptamer target. The excess sample reagent flows from the test line to the control line and to the absorbent pad eventually. Two slightly different LFAs have also been developed that use aptamers generated using Capture-SELEX. The LFA devised by Du et al. [24] combines lateral flow strips and the recombinase polymerase amplification technique for detecting erythromycin in tap water, whereas that devised by Xia et al. [89] uses aptamer EC1-34 as a recognition probe for detecting ethyl carbamate. The latter LFA differs from the former LFA only in terms of its use of a cationic polymer (such as poly(dimethyldiallylammonium chloride)) instead of streptavidin in the test line.

5. Biosensor Applications

5.1. Food Safety Analysis

5.1.1. Veterinary Drug Residues and Pesticides

Ractopamine (RAC) is a β -adrenergic agonist used illegally as an animal feed additive for increasing skeletal muscle mass, reducing fat deposition, and increasing protein accretion in livestock [125,126]. The accumulation of RAC in animals may increase the risk of food poisoning in humans and have other adverse effects on human health, such as causing headache, tachycardia, and muscle tremors [127]. Therefore, the development of a rapid and cost-effective biosensor for RAC contamination in food is warranted. Duan et al. [82] obtained nine aptamer candidates for RAC through 16 selection rounds of Capture-SELEX. The aptamer RAC-6 showed the highest binding affinity for RAC in a GO-based fluorescent assay, with weak binding affinity for other off-target species ($<22\%$). The researchers further developed a fluorescent aptasensor based on RAC-6 that exhibited a linear detection range of 0.33 to 331.79 nM, a low limit of detection (LOD; 0.13 nM; Table 2), and high recovery rates (82.57–104.65%). They found that RAC-6 was especially useful for detecting RAC contamination in pork samples.

λ -Cyhalothrin is a broad-spectrum pyrethroid insecticide used to control agricultural insect pests, such as Coleoptera, Lepidoptera, and mites, and thus increase agricultural productivity [128]. Compared with older-generation pesticides, the insecticidal effect of λ -cyhalothrin is 10–100 times stronger, and overuse of this insecticide may lead to food contamination [129]. Due to its toxicity, the ingestion of λ -cyhalothrin residues in food may cause serious adverse effects, including mouth ulcers, nausea, abdominal pain, and vomiting [130]. Yang et al. [76] used Capture-SELEX to obtain several candidate aptamers against λ -cyhalothrin. The aptamer LCT-1 showed the strongest affinity and

specificity for λ -cyhalothrin in a colorimetric assay and its binding affinity was further optimized by truncation. The dissociation constant of the truncated aptamer, named LCT-1-39, was improved by approximately 40 nM relative to LCT-1, and similar results were obtained using the MST assay. LCT-1 and LCT-1-39 were thus used to establish colorimetric aptasensors for detecting λ -cyhalothrin. These aptasensors demonstrated low LODs for LCT-1 and LCT-1-39 (43.8 nM and 41.35 nM, respectively; Table 2) and mean λ -cyhalothrin recovery rates of 82.93–95.50%. Compared with traditional quantification methods, these colorimetric aptasensors demonstrated more rapid detection of λ -cyhalothrin in cucumber and pear samples.

5.1.2. Food Additives and Flavoring Agents

Vanillin is the second most popular flavoring agent worldwide and is used as a food additive in sweet foods and beverages, and a masking agent in numerous pharmaceutical formulations [131]. It is a phenolic aldehyde that has demonstrated antioxidant, antimicrobial, and antifungal activities in various food products [132,133]. Hence, a rapid detection biosensor is required to monitor vanillin concentrations during processed food production. Through Capture-SELEX, Kuznetsov et al. [23] obtained six aptamer candidates against vanillin and found that Van_74 had the highest binding affinity by non-denaturing PAGE. Its specificity for vanillin was also confirmed in the presence of interferents, such as benzaldehyde, guaiacol, furaneol, ethyl guaiacol, and ethyl vanillin. The authors also found that Van_74 was sensitive to the composition of the selection buffer. Van_74 was then used in the development of an ion-sensitive field-effect transistor (ISFET)-based biosensor that demonstrated a low LOD (0.155 μ M) and a dynamic detection range of 0.155–1 μ M (Table 2). This novel aptasensor can be applied for the rapid on-site detection of vanillin contamination in coffee extracts and mixtures.

Another aroma compound, furaneol, is extensively used as an artificial flavoring agent as it imparts fruit flavor to food [134], and thus a rapid detection biosensor is required to monitor furaneol concentrations during processed food production. Komarova et al. [68] obtained eight aptamer candidates against furaneol through 13 selection rounds of Capture-SELEX. These aptamers' binding affinity for furaneol was analyzed by three methods: an exonuclease protection assay, an SGI assay, and an MB-associated elution assay. The results revealed that the aptamer Fur_14 had the highest binding affinity for furaneol; therefore, Fur_14 was used to develop an ISFET-based aptasensor. Fur_14 was further modified with an alkyne label at its 5'-end, and this Fur_14 derivative exhibited a furaneol detection range of 0.1–10 μ M (Table 2).

Spermine, tyramine (TYR), and β -phenethylamine (PHE) are biogenic amines (BAs) that are typically present in foodstuffs. As the consumption of foods containing high concentrations of BAs may cause toxic effects, biosensors are needed for BA detection in foods [135,136]. Tian et al. [44] obtained aptamer candidates against spermine by Capture-SELEX selection and tested them using ITC and fluorescence assays. The aptamer APJ-6 showed the highest affinity and specificity for spermine and was, thus, used to develop a fluorescent aptasensor for spermine detection in pork samples. This aptasensor demonstrated a linear detection range of 0.1–20 nM and a low LOD (0.052 nM). For detecting TYR and PHE, Kuznetsov et al. selected and isolated several aptamers using Capture-SELEX. The selection process was monitored by the melting temperature (T_m) in the screening process, and T_m peaked during the 14th round for both TYR and PHE. The aptamers TYR-2 and PHE-2 were identified to have the strongest binding affinity and specificity for TYR and PHE, respectively, based on a GO-based fluorescent assay. TYR-2 and PHE-2 were then used to develop fluorescent aptasensors for the detection of TYR and PHE in pork and bear meat samples. These aptasensors demonstrated LODs for TYR and PHE of 2.48 and 3.22 nM, respectively (Table 2), with target recovery rates in the range of 95.6–104.2%, suggesting their efficacy in detecting TYR and PHE in foods.

5.2. Aquatic Environment

5.2.1. Veterinary Drug Residues and Pesticides

Erythromycin is a broad-spectrum macrolide antibiotic used to treat diseases such as diphtheria, pertussis, and bacillary angiomatosis [137]. The natural degradation of erythromycin is prolonged due to its stable structure, leading to increased erythromycin resistance among bacteria [138]. As erythromycin diffuses rapidly into most tissues of the human body, erythromycin pollution of environmental media poses a serious threat to human health, in addition to the ecosystem. Du et al. [24] obtained 10 aptamer candidates against erythromycin through 20 selection rounds of Capture-SELEX. The binding affinity and specificity of the candidates were determined using an SGI fluorometric assay, an AuNP-based colorimetric assay, a quartz crystal microbalance with dissipation assay, and an agarose chasing diffusion assay, resulting in the selection of the aptamer Ery_06 for the development of a novel LFA. This LFA demonstrated an erythromycin-detection range of 250–500 pM in water samples, with a low LOD (3 pM; Table 2) and rapid detection (within 15 min), suggesting its efficacy for erythromycin detection in water.

Roxithromycin is a macrolide antibiotic that poses a similar risk to the ecosystem and human health as erythromycin, indicating the need to establish a rapid and effective detection device for monitoring roxithromycin residues in environmental media. Jiang et al. selected aptamer candidates against roxithromycin after 16 selection rounds of Capture-SELEX. The aptamer Ap01 demonstrated the highest affinity and specificity for roxithromycin, as indicated by the results of an SGI assay, and was therefore selected for the development of a colorimetric aptasensor for roxithromycin. The developed aptasensor demonstrated a low LOD (0.077 μ M) for roxithromycin in water samples (Table 2) and high recovery rates in the range of 90.48–109.39%.

5.2.2. Toxins and Plasticizers

Gymnodimines (GYMs) are fast-acting cyclic imine toxins that are biosynthesized by dinoflagellates and have deleterious effects on the aquatic environment with the accumulation. The contaminated environment can have serious toxic effects on filter feeding shellfish and thereby pose a threat to human health [139]. Zhang et al. [75] used Capture-SELEX to screen and obtain six aptamer candidates against gymnodimine-A (GYM-A). G48 exhibited the highest binding affinity (K_d : 288 nM) and was therefore chosen for further optimization and investigation. The truncated aptamer G48nop demonstrated an improved K_d value of 34.5 ± 1.72 nM and high specificity for GYM-A. A novel BLI-based aptasensor was established using this aptamer that detected GYM-A in the range of 55–1400 nM (linear range of 55–875 nM) and had a low LOD (6.21 nM; Table 2). This BLI-based aptasensor also demonstrated high recovery rates in the range of 96.65%–109.67%, indicating that is reliable and efficient in detecting and monitoring GYM-A in water samples.

Di(2-ethylhexyl) phthalate (DEHP) is a plasticizer that is widely used as an additive in packaging materials, and its residues are known to accumulate and dissolve in water [140]. DEHP is also a well-known endocrine disruptor that can enter the human body through ingestion of food or water and inhalation with contaminated air that disrupts the immune system. Lu et al. [71] selected aptamer candidates against DEHP through eight rounds of Capture-SELEX. Upon high-throughput sequencing and characterizing the candidate aptamers using an AuNP colorimetric assay and localized surface plasmon resonance, aptamer 31 was revealed to have high affinity and specificity. Aptamer 31 was thus used to develop an ultrasensitive electrochemical impedance spectroscopy aptasensor to detect DEHP in real water samples; this aptasensor demonstrated a low LOD (0.264 pM; Table 2) and a mean recovery rate ranging from 76.07% to 141.32%.

5.3. Other Potential Applications

Synthetic riboswitches can have several biotechnological applications, such as regulating gene expression, e.g., the construction of genetic circuits [141,142]. Natural riboswitches are mainly found in bacteria, while synthetic riboswitches are artificially generated by

combining aptamer domains (using in vitro SELEX method) with expression platforms to regulate gene expression via small-molecule-RNA interactions [143,144]. However, using the conventional SELEX method, only a ciprofloxacin riboswitch aptamer has been developed, as most aptamers have limitations, such as excellent binding affinity and conformation switching, and require cellular screening after in vitro selection [145]. Subsequently, Boussebayle et al. [146] identified a paromomycin riboswitch aptamer using Capture-SELEX and found it had a high affinity (K_d : 21 nM) using an ITC assay. Through further in vivo selection, this aptamer was revealed to have riboswitching properties. This work has introduced an efficient protocol for developing synthetic riboswitches and boosted the development of real-time intracellular biosensors for monitoring metabolic flows in living cells.

Zearalenone (ZEN) is a nonsteroidal estrogenic mycotoxin produced by fungi and is known to contaminate cereal grains and other crops [147]. Due to its high estrogenic activity, long-term intake of ZEN residues adversely affects human health by causing cervical cancer or hyperestrogenic syndrome [147,148]. Zhang et al. [84] obtained aptamer Z100 against ZEN after eight rounds of Capture-SELEX. Z100 was shown to have high affinity and specificity for ZEN in a fluorescence assay, and hence was selected to develop a rapid and on-site AuNP-based label-free aptasensor for detecting ZEN in agricultural produce. The developed aptasensor had a low LOD (12.5 nM), a linear detection range of 12.5–402.1 nM (Table 2), and high recovery rates in corn powder and feed (96.42–99.78% and 95.99–103.73%, respectively). This study revealed the great potential for developing aptamer-based inhibitors for ZEN to enhance animal feed safety.

Fenitrothion (FEN) is a broad-spectrum organophosphorus insecticide mainly used to control insect pests in agriculture [149]. As FEN is available at a low cost, large amounts of FEN are frequently applied in agriculture. High concentrations of FEN residues have been found in foods, which has become a great concern for human health and the environment. Trinh et al. [85] screened aptamer candidates against FEN through Capture-SELEX. In the thioflavin T (ThT) displacement assay, the aptamer FenA2 was identified to exhibit high-affinity FEN binding, as indicated by the loss of fluorescence. FenA2 was further optimized and used to develop a label-free ThT sensor. The developed aptasensor has a G4-quadruplex-like structure and a low LOD (14 nM; Table 2). This aptamer may be further optimized to develop a real-time FEN-detecting aptasensor.

6. Conclusions

Small-molecule contaminants are ubiquitous in the aquatic environment, agriculture produce, and animal feed due to the overuse of small molecules such as antibiotics and pesticides, and these contaminants pose a serious threat to human health and the environment. Owing to the few functional groups on these small molecules, screening aptamers against them is more challenging than doing so against large-molecule targets. Compared with other SELEX approaches, which involve the immobilization of small-molecule targets, the Capture-SELEX approach is more feasible, as they involve the immobilization of a biotinylated ssDNA/RNA library against which the binding affinity and specificity of small-molecule targets can be screened. To date, fewer than 50 studies have reported using Capture-SELEX to identify novel aptamers against specific small-molecule contaminants, suggesting that this process remains challenging, such as false-positive and lack of diversity. However, this research field has recently been receiving increasing attention from scientists. We hope that this review will encourage further research into the use of Capture-SELEX in generating aptamers against small-molecule contaminants. Six small-molecule aptamer characterization methods are introduced in this review. The high affinity and specificity aptamer work as a biorecognition element in aptasensor to detect specific small-molecule contaminants in environmental media and agricultural produce. This will help to improve food safety, aquatic environments, and agricultural crop production.

Author Contributions: Conceptualization, S.Y.L. and C.K.K.; writing—original draft preparation, S.Y.L. and C.K.K.; writing—review and editing, S.Y.L., H.L.L. and C.K.K.; visualization, S.Y.L. and C.K.K.; supervision, C.K.K.; funding acquisition, C.K.K. All authors have read and agreed to the published version of the manuscript.

Funding: This work was supported by the Shenzhen Basic Research Project [JCYJ20180507181642811]; National Natural Science Foundation of China Project [32222089]; Research Grants Council of the Hong Kong SAR, China Projects [CityU 11100222, CityU 11100421, CityU 11101519, CityU 11100218, N_CityU110/17]; Croucher Foundation Project [9509003]; State Key Laboratory of Marine Pollution Director Discretionary Fund; City University of Hong Kong projects [7005503, 9667222, 9680261] to C.K.K.

Institutional Review Board Statement: Not applicable.

Informed Consent Statement: Not applicable.

Data Availability Statement: Not applicable.

Acknowledgments: Not applicable.

Conflicts of Interest: The authors declare no conflict of interest.

References

1. Minh, T.B.; Leung, H.W.; Loi, I.H.; Chan, W.H.; So, M.K.; Mao, J.Q.; Choi, D.; Lam, J.C.; Martin, M.; Lee, J.H.W.; et al. Antibiotics in the Hong Kong metropolitan area: Ubiquitous distribution and fate in Victoria Harbour. *Mar. Pollut. Bull.* **2009**, *58*, 1052–1062. [[CrossRef](#)] [[PubMed](#)]
2. Gothwal, R.; Shashidhar, T. Antibiotic Pollution in the Environment: A Review. *CLEAN–Soil. Air Water* **2015**, *43*, 479–489. [[CrossRef](#)]
3. Parra-Arroyo, L.; Gonzalez-Gonzalez, R.B.; Castillo-Zacarias, C.; Melchor Martinez, E.M.; Sosa-Hernandez, J.E.; Bilal, M.; Iqbal, H.M.N.; Barcelo, D.; Parra-Saldivar, R. Highly hazardous pesticides and related pollutants: Toxicological, regulatory, and analytical aspects. *Sci. Total Environ.* **2022**, *807*, 151879. [[CrossRef](#)] [[PubMed](#)]
4. Pan, W.; Zeng, D.; Ding, N.; Luo, K.; Man, Y.B.; Zeng, L.; Zhang, Q.; Luo, J.; Kang, Y. Percutaneous Penetration and Metabolism of Plasticizers by Skin Cells and Its Implication in Dermal Exposure to Plasticizers by Skin Wipes. *Environ. Sci. Technol.* **2020**, *54*, 10181–10190. [[CrossRef](#)] [[PubMed](#)]
5. Eales, J.; Bethel, A.; Galloway, T.; Hopkinson, P.; Morrissey, K.; Short, R.E.; Garside, R. Human health impacts of exposure to phthalate plasticizers: An overview of reviews. *Environ. Int.* **2022**, *158*, 106903. [[CrossRef](#)]
6. Qadeer, A.; Kirsten, K.L.; Ajmal, Z.; Jiang, X.; Zhao, X. Alternative Plasticizers As Emerging Global Environmental and Health Threat: Another Regrettable Substitution? *Environ. Sci. Technol.* **2022**, *56*, 1482–1488. [[CrossRef](#)]
7. Schuster, C.; Sterz, S.; Teupser, D.; Brugel, M.; Vogeser, M.; Paal, M. Multiplex Therapeutic Drug Monitoring by Isotope-dilution HPLC-MS/MS of Antibiotics in Critical Illnesses. *J. Vis. Exp.* **2018**. [[CrossRef](#)]
8. Li, S.; Wnag, L.; Wu, J.; Inoue, H. Syntheses and spectra of Mn(III)-chlorophyll-a and Mn(II)-chlorophyll-a. *Guang Pu Xue Yu Guang Pu Fen Xi* **1997**, *17*, 55–59.
9. Sheng, W.; Xia, X.; Wei, K.; Li, J.; Li, Q.X.; Xu, T. Determination of marbofloxacin residues in beef and pork with an enzyme-linked immunosorbent assay. *J. Agric. Food Chem.* **2009**, *57*, 5971–5975. [[CrossRef](#)]
10. Wang, G.; Zhang, H.C.; Liu, J.; Wang, J.P. A receptor-based chemiluminescence enzyme linked immunosorbent assay for determination of tetracyclines in milk. *Anal. Biochem.* **2019**, *564–565*, 40–46. [[CrossRef](#)]
11. Dahal, U.P.; Jones, J.P.; Davis, J.A.; Rock, D.A. Small molecule quantification by liquid chromatography-mass spectrometry for metabolites of drugs and drug candidates. *Drug Metab. Dispos.* **2011**, *39*, 2355–2360. [[CrossRef](#)]
12. Li, B.; Van Schepdael, A.; Hoogmartens, J.; Adams, E. Characterization of impurities in tobramycin by liquid chromatography-mass spectrometry. *J. Chromatogr. A* **2009**, *1216*, 3941–3945. [[CrossRef](#)]
13. Zhou, J.; Rossi, J. Aptamers as targeted therapeutics: Current potential and challenges. *Nat. Rev. Drug Discov.* **2017**, *16*, 440. [[CrossRef](#)]
14. Thiviyanathan, V.; Gorenstein, D.G. Aptamers and the next generation of diagnostic reagents. *Proteom. Clin. Appl.* **2012**, *6*, 563–573. [[CrossRef](#)]
15. He, Y.; Zhou, L.; Deng, L.; Feng, Z.; Cao, Z.; Yin, Y. An electrochemical impedimetric sensing platform based on a peptide aptamer identified by high-throughput molecular docking for sensitive l-arginine detection. *Bioelectrochemistry* **2021**, *137*, 107634. [[CrossRef](#)]
16. Lin, N.; Wu, L.; Xu, X.; Wu, Q.; Wang, Y.; Shen, H.; Song, Y.; Wang, H.; Zhu, Z.; Kang, D.; et al. Aptamer Generated by Cell-SELEX for Specific Targeting of Human Glioma Cells. *ACS Appl. Mater. Interfaces* **2021**, *13*, 9306–9315. [[CrossRef](#)]
17. Chen, X.; Qiu, L.; Cai, R.; Cui, C.; Li, L.; Jiang, J.H.; Tan, W. Aptamer-Directed Protein-Specific Multiple Modifications of Membrane Glycoproteins on Living Cells. *ACS Appl. Mater. Interfaces* **2020**, *12*, 37845–37850. [[CrossRef](#)]

18. Lohlamoh, W.; Soontornworajit, B.; Rotkrua, P. Anti-Proliferative Effect of Doxorubicin-Loaded AS1411 Aptamer on Colorectal Cancer Cell. *Asian Pac. J. Cancer Prev.* **2021**, *22*, 2209–2219. [[CrossRef](#)]
19. Amraee, M.; Oloomi, M.; Yavari, A.; Bouzari, S. DNA aptamer identification and characterization for E. coli O157 detection using cell based SELEX method. *Anal. Biochem.* **2017**, *536*, 36–44. [[CrossRef](#)]
20. Chinnappan, R.; Eissa, S.; Alotaibi, A.; Siddiqua, A.; Alsager, O.A.; Zourob, M. In vitro selection of DNA aptamers and their integration in a competitive voltammetric biosensor for azlocillin determination in waste water. *Anal. Chim. Acta* **2020**, *1101*, 149–156. [[CrossRef](#)]
21. Paniel, N.; Istamboulie, G.; Triki, A.; Lozano, C.; Barthelmebs, L.; Noguier, T. Selection of DNA aptamers against penicillin G using Capture-SELEX for the development of an impedimetric sensor. *Talanta* **2017**, *162*, 232–240. [[CrossRef](#)] [[PubMed](#)]
22. Stoltenburg, R.; Nikolaus, N.; Strehlitz, B. Capture-SELEX: Selection of DNA Aptamers for Aminoglycoside Antibiotics. *J. Anal. Methods Chem.* **2012**, *2012*, 415697. [[CrossRef](#)] [[PubMed](#)]
23. Kuznetsov, A.; Komarova, N.; Andrianova, M.; Grudtsov, V.; Kuznetsov, E. Aptamer based vanillin sensor using an ion-sensitive field-effect transistor. *Mikrochim. Acta* **2017**, *185*, 3. [[CrossRef](#)] [[PubMed](#)]
24. Du, Y.; Liu, D.; Wang, M.; Guo, F.; Lin, J.S. Preparation of DNA aptamer and development of lateral flow aptasensor combining recombinase polymerase amplification for detection of erythromycin. *Biosens. Bioelectron.* **2021**, *181*, 113157. [[CrossRef](#)] [[PubMed](#)]
25. Tuerk, C.; Gold, L. Systematic evolution of ligands by exponential enrichment: RNA ligands to bacteriophage T4 DNA polymerase. *Science* **1990**, *249*, 505–510. [[CrossRef](#)]
26. Ellington, A.D.; Szostak, J.W. In vitro selection of RNA molecules that bind specific ligands. *Nature* **1990**, *346*, 818–822. [[CrossRef](#)]
27. Robertson, D.L.; Joyce, G.F. Selection in vitro of an RNA enzyme that specifically cleaves single-stranded DNA. *Nature* **1990**, *344*, 467–468. [[CrossRef](#)]
28. Yang, J.; Bowser, M.T. Capillary electrophoresis-SELEX selection of catalytic DNA aptamers for a small-molecule porphyrin target. *Anal. Chem.* **2013**, *85*, 1525–1530. [[CrossRef](#)]
29. Eaton, R.M.; Shallcross, J.A.; Mael, L.E.; Mears, K.S.; Minkoff, L.; Scoville, D.J.; Whelan, R.J. Selection of DNA aptamers for ovarian cancer biomarker HE4 using CE-SELEX and high-throughput sequencing. *Anal. Bioanal. Chem.* **2015**, *407*, 6965–6973. [[CrossRef](#)]
30. Zhu, C.; Li, L.; Fang, S.; Zhao, Y.; Zhao, L.; Yang, G.; Qu, F. Selection and characterization of an ssDNA aptamer against thyroglobulin. *Talanta* **2021**, *223*, 121690. [[CrossRef](#)]
31. Kou, Q.; Wu, P.; Sun, Q.; Li, C.; Zhang, L.; Shi, H.; Wu, J.; Wang, Y.; Yan, X.; Le, T. Selection and truncation of aptamers for ultrasensitive detection of sulfamethazine using a fluorescent biosensor based on graphene oxide. *Anal. Bioanal. Chem.* **2021**, *413*, 901–909. [[CrossRef](#)]
32. Ozyurt, C.; Canbay, Z.C.; Dinckaya, E.; Evran, S. A highly sensitive DNA aptamer-based fluorescence assay for sarcosine detection down to picomolar levels. *Int. J. Biol. Macromol.* **2019**, *129*, 91–97. [[CrossRef](#)]
33. Kim, S.H.; Lee, J.; Lee, B.H.; Song, C.S.; Gu, M.B. Specific detection of avian influenza H5N2 whole virus particles on lateral flow strips using a pair of sandwich-type aptamers. *Biosens. Bioelectron.* **2019**, *134*, 123–129. [[CrossRef](#)]
34. Wang, G.; Liu, J.; Chen, K.; Xu, Y.; Liu, B.; Liao, J.; Zhu, L.; Hu, X.; Li, J.; Pu, Y.; et al. Selection and characterization of DNA aptamer against glucagon receptor by cell-SELEX. *Sci. Rep.* **2017**, *7*, 7179. [[CrossRef](#)]
35. Yilmaz, D.; Muslu, T.; Parlar, A.; Kurt, H.; Yuca, M. SELEX against whole-cell bacteria resulted in lipopolysaccharide binding aptamers. *J. Biotechnol.* **2022**, *354*, 10–20. [[CrossRef](#)]
36. Wan, J.; Ye, L.; Yang, X.; Guo, Q.; Wang, K.; Huang, Z.; Tan, Y.; Yuan, B.; Xie, Q. Cell-SELEX based selection and optimization of DNA aptamers for specific recognition of human cholangiocarcinoma QBC-939 cells. *Analyst* **2015**, *140*, 5992–5997. [[CrossRef](#)]
37. Wang, H.; Zhang, Y.; Yang, H.; Qin, M.; Ding, X.; Liu, R.; Jiang, Y. In Vivo SELEX of an Inhibitory NSCLC-Specific RNA Aptamer from PEGylated RNA Library. *Mol. Ther. Nucleic Acids* **2018**, *10*, 187–198. [[CrossRef](#)]
38. Huang, X.; Zhong, J.; Ren, J.; Wen, D.; Zhao, W.; Huan, Y. A DNA aptamer recognizing MMP14 for in vivo and in vitro imaging identified by cell-SELEX. *Oncol. Lett.* **2019**, *18*, 265–274. [[CrossRef](#)]
39. Reinemann, C.; Freiin von Fritsch, U.; Rudolph, S.; Strehlitz, B. Generation and characterization of quinolone-specific DNA aptamers suitable for water monitoring. *Biosens. Bioelectron.* **2016**, *77*, 1039–1047. [[CrossRef](#)]
40. Stoltenburg, R.; Reinemann, C.; Strehlitz, B. FluMag-SELEX as an advantageous method for DNA aptamer selection. *Anal. Bioanal. Chem.* **2005**, *383*, 83–91. [[CrossRef](#)]
41. Lyu, C.; Khan, I.M.; Wang, Z. Capture-SELEX for aptamer selection: A short review. *Talanta* **2021**, *229*, 122274. [[CrossRef](#)] [[PubMed](#)]
42. Jenison, R.D.; Gill, S.C.; Pardi, A.; Polisky, B. High-resolution molecular discrimination by RNA. *Science* **1994**, *263*, 1425–1429. [[CrossRef](#)]
43. Shkemi, X.; Skouridou, V.; Svobodova, M.; Leonardo, S.; Bashammakh, A.S.; Alyoubi, A.O.; Campas, M.; CK, O.S. Hybrid Antibody-Aptamer Assay for Detection of Tetrodotoxin in Pufferfish. *Anal. Chem.* **2021**. [[CrossRef](#)] [[PubMed](#)]
44. Tian, H.; Duan, N.; Wu, S.; Wang, Z. Selection and application of ssDNA aptamers against spermine based on Capture-SELEX. *Anal. Chim. Acta* **2019**, *1081*, 168–175. [[CrossRef](#)] [[PubMed](#)]
45. Song, M.; Lyu, C.; Duan, N.; Wu, S.; Khan, I.M.; Wang, Z. The isolation of high-affinity ssDNA aptamer for the detection of ribavirin in chicken. *Anal. Methods* **2021**, *13*, 3110–3117. [[CrossRef](#)]

46. Wang, T.; Chen, C.; Larcher, L.M.; Barrero, R.A.; Veedu, R.N. Three decades of nucleic acid aptamer technologies: Lessons learned, progress and opportunities on aptamer development. *Biotechnol. Adv.* **2019**, *37*, 28–50. [[CrossRef](#)]
47. Spiga, F.M.; Maietta, P.; Guiducci, C. More DNA-Aptamers for Small Drugs: A Capture-SELEX Coupled with Surface Plasmon Resonance and High-Throughput Sequencing. *ACS Comb. Sci.* **2015**, *17*, 326–333. [[CrossRef](#)]
48. Sanger, F.; Nicklen, S.; Coulson, A.R. DNA sequencing with chain-terminating inhibitors. *Proc. Natl. Acad. Sci. USA* **1977**, *74*, 5463–5467. [[CrossRef](#)]
49. Crossley, B.M.; Bai, J.; Glaser, A.; Maes, R.; Porter, E.; Killian, M.L.; Clement, T.; Toohey-Kurth, K. Guidelines for Sanger sequencing and molecular assay monitoring. *J. Vet. Diagn. Investig.* **2020**, *32*, 767–775. [[CrossRef](#)]
50. Levy, S.E.; Myers, R.M. Advancements in Next-Generation Sequencing. *Annu. Rev. Genom. Hum. Genet.* **2016**, *17*, 95–115. [[CrossRef](#)]
51. Balasubramanian, S. Solexa sequencing: Decoding genomes on a population scale. *Clin. Chem.* **2015**, *61*, 21–24. [[CrossRef](#)]
52. Slatko, B.E.; Gardner, A.F.; Ausubel, F.M. Overview of Next-Generation Sequencing Technologies. *Curr. Protoc. Mol. Biol.* **2018**, *122*, e59. [[CrossRef](#)]
53. Eisold, A.; Labudde, D. Detailed Analysis of 17beta-Estradiol-Aptamer Interactions: A Molecular Dynamics Simulation Study. *Molecules* **2018**, *23*, 1690. [[CrossRef](#)]
54. Bavi, R.; Liu, Z.; Han, Z.; Zhang, H.; Gu, Y. In silico designed RNA aptamer against epithelial cell adhesion molecule for cancer cell imaging. *Biochem. Biophys. Res. Commun.* **2019**, *509*, 937–942. [[CrossRef](#)]
55. Ahmad, N.A.; Mohamed Zulkifli, R.; Hussin, H.; Nadri, M.H. In silico approach for Post-SELEX DNA aptamers: A mini-review. *J. Mol. Graph Model* **2021**, *105*, 107872. [[CrossRef](#)]
56. Larkin, M.A.; Blackshields, G.; Brown, N.P.; Chenna, R.; McGettigan, P.A.; McWilliam, H.; Valentin, F.; Wallace, I.M.; Wilm, A.; Lopez, R.; et al. Clustal W and Clustal X version 2.0. *Bioinformatics* **2007**, *23*, 2947–2948. [[CrossRef](#)]
57. Sievers, F.; Higgins, D.G. Clustal omega. *Curr. Protoc. Bioinform.* **2014**, *48*, 3–13. [[CrossRef](#)]
58. Bailey, T.L.; Boden, M.; Buske, F.A.; Frith, M.; Grant, C.E.; Clementi, L.; Ren, J.; Li, W.W.; Noble, W.S. MEME SUITE: Tools for motif discovery and searching. *Nucleic Acids Res.* **2009**, *37*, W202–W208. [[CrossRef](#)]
59. Zuker, M. Mfold web server for nucleic acid folding and hybridization prediction. *Nucleic Acids Res.* **2003**, *31*, 3406–3415. [[CrossRef](#)]
60. Xayaphoummine, A.; Bucher, T.; Isambert, H. Kinefold web server for RNA/DNA folding path and structure prediction including pseudoknots and knots. *Nucleic Acids Res.* **2005**, *33*, W605–W610. [[CrossRef](#)]
61. Xu, Z.Z.; Mathews, D.H. Experiment-Assisted Secondary Structure Prediction with RNAstructure. *Methods Mol. Biol.* **2016**, *1490*, 163–176. [[CrossRef](#)] [[PubMed](#)]
62. Chen, Z.; Hu, L.; Zhang, B.T.; Lu, A.; Wang, Y.; Yu, Y.; Zhang, G. Artificial Intelligence in Aptamer-Target Binding Prediction. *Int. J. Mol. Sci.* **2021**, *22*, 3605. [[CrossRef](#)] [[PubMed](#)]
63. Soon, S.; Nordin, N.A. In silico predictions and optimization of aptamers against streptococcus agalactiae surface protein using computational docking. *Mater. Today-Proc.* **2019**, *16*, 2096–2100. [[CrossRef](#)]
64. Douaki, A.; Garoli, D.; Inam, A.; Angeli, M.A.C.; Cantarella, G.; Rocchia, W.; Wang, J.; Petti, L.; Lugli, P. Smart Approach for the Design of Highly Selective Aptamer-Based Biosensors. *Biosensors* **2022**, *12*, 574. [[CrossRef](#)] [[PubMed](#)]
65. Mousivand, M.; Anfossi, L.; Bagherzadeh, K.; Barbero, N.; Mirzadi-Gohari, A.; Javan-Nikkhah, M. In silico maturation of affinity and selectivity of DNA aptamers against aflatoxin B1 for biosensor development. *Anal. Chim. Acta* **2020**, *1105*, 178–186. [[CrossRef](#)]
66. Kadam, U.S.; Hong, J.C. Advances in aptamer biosensors designed to detect toxic contaminants from food, water, human fluids, and the environment. *Trends Environ. Anal. Chem.* **2022**, *36*, e00184. [[CrossRef](#)]
67. Tian, Y.; Wang, Y.; Sheng, Z.; Li, T.; Li, X. A colorimetric detection method of pesticide acetamiprid by fine-tuning aptamer length. *Anal. Biochem.* **2016**, *513*, 87–92. [[CrossRef](#)]
68. Komarova, N.; Andrianova, M.; Glukhov, S.; Kuznetsov, A. Selection, Characterization, and Application of ssDNA Aptamer against Furaneol. *Molecules* **2018**, *23*, 3159. [[CrossRef](#)]
69. Song, M.; Li, C.; Wu, S.; Duan, N. Screening of specific aptamers against chlorpromazine and construction of novel ratiometric fluorescent aptasensor based on metal-organic framework. *Talanta* **2022**, *252*, 123850. [[CrossRef](#)]
70. Jiang, L.; Wang, M.; Zhang, Y.; Chen, H.; Su, Y.; Wang, Y.; Lin, J.S. Preparation and characterization of DNA aptamers against roxithromycin. *Anal. Chim. Acta* **2021**, *1164*, 338509. [[CrossRef](#)]
71. Lu, Q.; Liu, X.; Hou, J.; Yuan, Q.; Li, Y.; Chen, S. Selection of Aptamers Specific for DEHP Based on ssDNA Library Immobilized SELEX and Development of Electrochemical Impedance Spectroscopy Aptasensor. *Molecules* **2020**, *25*, 747. [[CrossRef](#)]
72. Ren, L.; Qi, S.; Khan, I.M.; Wu, S.; Duan, N.; Wang, Z. Screening and application of a broad-spectrum aptamer for acyclic guanosine analogues. *Anal. Bioanal. Chem.* **2021**, *413*, 4855–4863. [[CrossRef](#)]
73. Wu, C.; Barkova, D.; Komarova, N.; Offenhausser, A.; Andrianova, M.; Hu, Z.; Kuznetsov, A.; Mayer, D. Highly selective and sensitive detection of glutamate by an electrochemical aptasensor. *Anal. Bioanal. Chem.* **2021**, *414*, 1609–1622. [[CrossRef](#)]
74. Li, C.; Song, M.; Wu, S.; Wang, Z.; Duan, N. Selection of aptamer targeting levamisole and development of a colorimetric and SERS dual-mode aptasensor based on AuNPs/Cu-TCPP(Fe) nanosheets. *Talanta* **2023**, *251*, 123739. [[CrossRef](#)]
75. Zhang, X.; Gao, Y.; Deng, B.; Hu, B.; Zhao, L.; Guo, H.; Yang, C.; Ma, Z.; Sun, M.; Jiao, B.; et al. Selection, Characterization, and Optimization of DNA Aptamers against Challenging Marine Biotxin Gymnodimine-A for Biosensing Application. *Toxins* **2022**, *14*, 195. [[CrossRef](#)]

76. Yang, Y.; Tang, Y.; Wang, C.; Liu, B.; Wu, Y. Selection and identification of a DNA aptamer for ultrasensitive and selective detection of lambda-cyhalothrin residue in food. *Anal. Chim. Acta* **2021**, *1179*, 338837. [[CrossRef](#)]
77. Xie, M.; Chen, Z.; Zhao, F.; Lin, Y.; Zheng, S.; Han, S. Selection and Application of ssDNA Aptamers for Fluorescence Biosensing Detection of Malachite Green. *Foods* **2022**, *11*, 801. [[CrossRef](#)]
78. Wu, W.; Sun, Q.; Li, T.; Liu, K.; Jiang, Y.; Wang, Y.; Yang, Y. Selection and characterization of bispecific aptamers against malachite green and leucomalachite green. *Anal. Biochem.* **2022**, *658*, 114849. [[CrossRef](#)]
79. Wang, L.; Liu, X.; Zhang, Q.; Zhang, C.; Liu, Y.; Tu, K.; Tu, J. Selection of DNA aptamers that bind to four organophosphorus pesticides. *Biotechnol. Lett.* **2012**, *34*, 869–874. [[CrossRef](#)]
80. Martin, J.A.; Chavez, J.L.; Chushak, Y.; Chapleau, R.R.; Hagen, J.; Kelley-Loughnane, N. Tunable stringency aptamer selection and gold nanoparticle assay for detection of cortisol. *Anal. Bioanal. Chem.* **2014**, *406*, 4637–4647. [[CrossRef](#)]
81. Duan, N.; Gong, W.; Wu, S.; Wang, Z. Selection and Application of ssDNA Aptamers against Clenbuterol Hydrochloride Based on ssDNA Library Immobilized SELEX. *J. Agric. Food Chem.* **2017**, *65*, 1771–1777. [[CrossRef](#)] [[PubMed](#)]
82. Duan, N.; Gong, W.; Wu, S.; Wang, Z. An ssDNA library immobilized SELEX technique for selection of an aptamer against ractopamine. *Anal. Chim. Acta* **2017**, *961*, 100–105. [[CrossRef](#)] [[PubMed](#)]
83. Abraham, K.M.; Roueinfar, M.; Ponce, A.T.; Lussier, M.E.; Benson, D.B.; Hong, K.L. In Vitro Selection and Characterization of a Single-Stranded DNA Aptamer Against the Herbicide Atrazine. *ACS Omega* **2018**, *3*, 13576–13583. [[CrossRef](#)]
84. Zhang, Y.; Lu, T.; Wang, Y.; Diao, C.; Zhou, Y.; Zhao, L.; Chen, H. Selection of a DNA Aptamer against Zearalenone and Docking Analysis for Highly Sensitive Rapid Visual Detection with Label-Free Aptasensor. *J. Agric. Food Chem.* **2018**, *66*, 12102–12110. [[CrossRef](#)] [[PubMed](#)]
85. Trinh, K.H.; Kadam, U.S.; Song, J.; Cho, Y.; Kang, C.H.; Lee, K.O.; Lim, C.O.; Chung, W.S.; Hong, J.C. Novel DNA Aptameric Sensors to Detect the Toxic Insecticide Fenitrothion. *Int. J. Mol. Sci.* **2021**, *22*, 846. [[CrossRef](#)] [[PubMed](#)]
86. Kadam, U.S.; Trinh, K.H.; Kumar, V.; Lee, K.W.; Cho, Y.; Can, M.T.; Lee, H.; Kim, Y.; Kim, S.; Kang, J.; et al. Identification and structural analysis of novel malathion-specific DNA aptameric sensors designed for food testing. *Biomaterials* **2022**, *287*, 121617. [[CrossRef](#)]
87. Trinh, K.H.; Kadam, U.S.; Rampogu, S.; Cho, Y.; Yang, K.A.; Kang, C.H.; Lee, K.W.; Lee, K.O.; Chung, W.S.; Hong, J.C. Development of novel fluorescence-based and label-free noncanonical G4-quadruplex-like DNA biosensor for facile, specific, and ultrasensitive detection of fipronil. *J. Hazard Mater.* **2022**, *427*, 127939. [[CrossRef](#)]
88. Can, M.T.; Kadam, U.S.; Trinh, K.H.; Cho, Y.; Lee, H.; Kim, Y.; Kim, S.; Kang, C.H.; Kim, S.H.; Chung, W.S.; et al. Engineering Novel Aptameric Fluorescent Biosensors for Analysis of the Neurotoxic Environmental Contaminant Insecticide Diazinon from Real Vegetable and Fruit Samples. *Front Biosci. (Landmark Ed.)* **2022**, *27*, 92. [[CrossRef](#)]
89. Xia, L.; Yang, Y.; Yang, H.; Tang, Y.; Zhou, J.; Wu, Y. Screening and identification of an aptamer as novel recognition molecule in the test strip and its application for visual detection of ethyl carbamate in liquor. *Anal. Chim. Acta* **2022**, *1226*, 340289. [[CrossRef](#)]
90. Yu, H.; Yang, W.; Alkhamis, O.; Canoura, J.; Yang, K.A.; Xiao, Y. In vitro isolation of small-molecule-binding aptamers with intrinsic dye-displacement functionality. *Nucleic Acids Res.* **2018**, *46*, e43. [[CrossRef](#)]
91. Zhang, W.; Li, D.; Zhang, J.; Jiang, L.; Li, Z.; Lin, J.S. Preparation and Characterization of Aptamers Against O,p'-DDT. *Int. J. Mol. Sci.* **2020**, *21*, 2211. [[CrossRef](#)]
92. Matsenko, N.U.; Rijikova, V.S.; Kovalenko, S.P. Comparison of SYBR Green I and TaqMan real-time PCR formats for the analysis of her2 gene dose in human breast tumors. *Bull. Exp. Biol. Med.* **2008**, *145*, 240–244. [[CrossRef](#)]
93. Marinowic, D.R.; Zanirati, G.; Rodrigues, F.V.F.; Grahl, M.V.C.; Alcará, A.M.; Machado, D.C.; Da Costa, J.C. A new SYBR Green real-time PCR to detect SARS-CoV-2. *Sci. Rep.* **2021**, *11*, 2224. [[CrossRef](#)]
94. Schnerr, H.; Niessen, L.; Vogel, R.F. Real time detection of the tri5 gene in Fusarium species by lightcycler-PCR using SYBR Green I for continuous fluorescence monitoring. *Int. J. Food Microbiol.* **2001**, *71*, 53–61. [[CrossRef](#)]
95. Vitzthum, F.; Geiger, G.; Bisswanger, H.; Brunner, H.; Bernhagen, J. A quantitative fluorescence-based microplate assay for the determination of double-stranded DNA using SYBR Green I and a standard ultraviolet transilluminator gel imaging system. *Anal. Biochem.* **1999**, *276*, 59–64. [[CrossRef](#)]
96. Iida, R.; Yasuda, T.; Tsubota, E.; Nakashima, Y.; Sawazaki, K.; Aoyama, M.; Matsuki, T.; Kishi, K. Detection of isozymes of deoxyribonucleases I and II on electrophoresed gels with picogram sensitivity using SYBR Green I. *Electrophoresis* **1998**, *19*, 2416–2418. [[CrossRef](#)]
97. Izumiyama, S.; Omura, M.; Takasaki, T.; Ohmae, H.; Asahi, H. Plasmodium falciparum: Development and validation of a measure of intraerythrocytic growth using SYBR Green I in a flow cytometer. *Exp. Parasitol.* **2009**, *121*, 144–150. [[CrossRef](#)]
98. Assuncao, P.; Rosales, R.S.; Rifatbegovic, M.; Antunes, N.T.; de la Fe, C.; Ruiz de Galarreta, C.M.; Poveda, J.B. Quantification of mycoplasmas in broth medium with sybr green-I and flow cytometry. *Front. Biosci.* **2006**, *11*, 492–497. [[CrossRef](#)]
99. Dragan, A.I.; Pavlovic, R.; McGivney, J.B.; Casas-Finet, J.R.; Bishop, E.S.; Strouse, R.J.; Schenerman, M.A.; Geddes, C.D. SYBR Green I: Fluorescence properties and interaction with DNA. *J. Fluoresc.* **2012**, *22*, 1189–1199. [[CrossRef](#)]
100. Wang, Y.; Bao, L.; Liu, Z.; Pang, D.W. Aptamer biosensor based on fluorescence resonance energy transfer from upconverting phosphors to carbon nanoparticles for thrombin detection in human plasma. *Anal. Chem.* **2011**, *83*, 8130–8137. [[CrossRef](#)]
101. Li, H.L.; Zhang, Y.W.; Wang, L.; Tian, J.Q.; Sun, X.P. Nucleic acid detection using carbon nanoparticles as a fluorescent sensing platform. *Chem. Commun.* **2011**, *47*, 961–963. [[CrossRef](#)]

102. Kimling, J.; Maier, M.; Okenve, B.; Kotaidis, V.; Ballot, H.; Plech, A. Turkevich method for gold nanoparticle synthesis revisited. *J. Phys. Chem. B* **2006**, *110*, 15700–15707. [[CrossRef](#)] [[PubMed](#)]
103. Wu, Y.; Zhan, S.; Wang, L.; Zhou, P. Selection of a DNA aptamer for cadmium detection based on cationic polymer mediated aggregation of gold nanoparticles. *Analyst* **2014**, *139*, 1550–1561. [[CrossRef](#)] [[PubMed](#)]
104. Alba-Molina, D.; Martin-Romero, M.T.; Camacho, L.; Giner-Casares, J.J. Ion-Mediated Aggregation of Gold Nanoparticles for Light-Induced Heating. *Appl. Sci.* **2017**, *7*, 916. [[CrossRef](#)]
105. Zhao, W.; Chiuman, W.; Lam, J.C.; McManus, S.A.; Chen, W.; Cui, Y.; Pelton, R.; Brook, M.A.; Li, Y. DNA aptamer folding on gold nanoparticles: From colloid chemistry to biosensors. *J. Am. Chem. Soc.* **2008**, *130*, 3610–3618. [[CrossRef](#)] [[PubMed](#)]
106. Smith, A.T.; LaChance, A.M.; Zeng, S.; Liu, B.; Sun, L. Synthesis, properties, and applications of graphene oxide/reduced graphene oxide and their nanocomposites. *Nano Mater. Sci.* **2019**, *1*, 31–47. [[CrossRef](#)]
107. Offeman, W.S.H.J.a.R.E. Preparation of Graphitic Oxide. *J. Am. Chem. Soc.* **1958**, *80*, 1339. [[CrossRef](#)]
108. Lakowicz, J.R.; Weber, G. Quenching of fluorescence by oxygen. A probe for structural fluctuations in macromolecules. *Biochemistry* **1973**, *12*, 4161–4170. [[CrossRef](#)]
109. Duan, N.; Song, M.; Mi, W.; Wang, Z.; Wu, S. Effectively Selecting Aptamers for Targeting Aromatic Biogenic Amines and Their Application in Aptasensing Establishment. *J. Agric. Food Chem.* **2021**. [[CrossRef](#)]
110. Lin, K.; Wu, G. Isothermal Titration Calorimetry Assays to Measure Binding Affinities In Vitro. *Methods Mol. Biol.* **2019**, *1893*, 257–272. [[CrossRef](#)]
111. Wang, H.; Cheng, H.; Wang, J.; Xu, L.; Chen, H.; Pei, R. Selection and characterization of DNA aptamers for the development of light-up biosensor to detect Cd(II). *Talanta* **2016**, *154*, 498–503. [[CrossRef](#)]
112. Overacker, R.D.; Plitzko, B.; Loesgen, S. Biolayer interferometry provides a robust method for detecting DNA binding small molecules in microbial extracts. *Anal. Bioanal. Chem.* **2021**, *413*, 1159–1171. [[CrossRef](#)]
113. Ciesielski, G.L.; Hytonen, V.P.; Kaguni, L.S. Biolayer Interferometry: A Novel Method to Elucidate Protein-Protein and Protein-DNA Interactions in the Mitochondrial DNA Replisome. *Methods Mol. Biol.* **2016**, *1351*, 223–231. [[CrossRef](#)]
114. Teague, J.L.; Barrows, J.K.; Baafi, C.A.; Van Dyke, M.W. Discovering the DNA-Binding Consensus of the Thermus thermophilus HB8 Transcriptional Regulator TTHA1359. *Int. J. Mol. Sci.* **2021**, *22*, 42. [[CrossRef](#)]
115. Kamat, V.; Rafique, A. Designing binding kinetic assay on the bio-layer interferometry (BLI) biosensor to characterize antibody-antigen interactions. *Anal. Biochem.* **2017**, *536*, 16–31. [[CrossRef](#)]
116. Wartchow, C.A.; Podlaski, F.; Li, S.; Rowan, K.; Zhang, X.; Mark, D.; Huang, K.S. Biosensor-based small molecule fragment screening with biolayer interferometry. *J. Comput. Aided Mol. Des.* **2011**, *25*, 669–676. [[CrossRef](#)]
117. Cusano, A.M.; Aliberti, A.; Cusano, A.; Ruvo, M. Detection of small DNA fragments by biolayer interferometry. *Anal. Biochem.* **2020**, *607*, 113898. [[CrossRef](#)]
118. Mahmoudinobar, F.; Britton, D.; Montclare, J.K. Protein-based lateral flow assays for COVID-19 detection. *Protein Eng. Des. Sel.* **2021**, *34*, gzab010. [[CrossRef](#)]
119. Sachdeva, S.; Davis, R.W.; Saha, A.K. Microfluidic Point-of-Care Testing: Commercial Landscape and Future Directions. *Front. Bioeng. Biotechnol.* **2020**, *8*, 602659. [[CrossRef](#)]
120. Boehringer, H.R.; O’Farrell, B.J. Lateral Flow Assays in Infectious Disease Diagnosis. *Clin. Chem.* **2021**, *68*, 52–58. [[CrossRef](#)]
121. Wang, L.; Wang, R.; Wei, H.; Li, Y. Selection of aptamers against pathogenic bacteria and their diagnostics application. *World J. Microbiol. Biotechnol.* **2018**, *34*, 149. [[CrossRef](#)] [[PubMed](#)]
122. Zhu, C.; Zhao, Y.; Yan, M.; Huang, Y.; Yan, J.; Bai, W.; Chen, A. A sandwich dipstick assay for ATP detection based on split aptamer fragments. *Anal. Bioanal. Chem.* **2016**, *408*, 4151–4158. [[CrossRef](#)] [[PubMed](#)]
123. Wang, T.; Chen, L.; Chikkanna, A.; Chen, S.; Brusius, I.; Sbuh, N.; Veedu, R.N. Development of nucleic acid aptamer-based lateral flow assays: A robust platform for cost-effective point-of-care diagnosis. *Theranostics* **2021**, *11*, 5174–5196. [[CrossRef](#)] [[PubMed](#)]
124. Petrakova, A.V.; Urusov, A.E.; Zherdev, A.V.; Dzantiev, B.B. Gold nanoparticles of different shape for bicolor lateral flow test. *Anal. Biochem.* **2019**, *568*, 7–13. [[CrossRef](#)] [[PubMed](#)]
125. Mohammadi, M.; Abazari, M.; Nourozi, M. Effects of two beta-adrenergic agonists on adipose tissue, plasma hormones and metabolites of Moghani ewes. *Small Ruminant. Res.* **2006**, *63*, 84–90. [[CrossRef](#)]
126. Fan, F.S. Assessing the Possible Influence of Residues of Ractopamine, a Livestock Feed Additive, in Meat on Alzheimer Disease. *Dement. Geriatr. Cogn. Dis. Extra* **2021**, *11*, 110–113. [[CrossRef](#)]
127. Wang, M.Y.; Zhu, W.; Ma, L.; Ma, J.J.; Zhang, D.E.; Tong, Z.W.; Chen, J. Enhanced simultaneous detection of ractopamine and salbutamol—Via electrochemical-facial deposition of MnO₂ nanoflowers onto 3D RGO/Ni foam templates. *Biosens. Bioelectron.* **2016**, *78*, 259–266. [[CrossRef](#)]
128. Bownik, A.; Kowalczyk, M.; Banczerowski, J. Lambda-cyhalothrin affects swimming activity and physiological responses of *Daphnia magna*. *Chemosphere* **2019**, *216*, 805–811. [[CrossRef](#)]
129. Djouaka, R.; Soglo, M.F.; Kusimo, M.O.; Adeoti, R.; Talom, A.; Zeukeng, F.; Paraiso, A.; Afari-Sefa, V.; Saethre, M.G.; Manyong, V.; et al. The Rapid Degradation of Lambda-Cyhalothrin Makes Treated Vegetables Relatively Safe for Consumption. *Int. J. Environ. Res. Public Health* **2018**, *15*, 1536. [[CrossRef](#)]
130. Bradberry, S.M.; Cage, S.A.; Proudfoot, A.T.; Vale, J.A. Poisoning due to pyrethroids. *Toxicol. Rev.* **2005**, *24*, 93–106. [[CrossRef](#)]
131. Banerjee, G.; Chattopadhyay, P. Vanillin biotechnology: The perspectives and future. *J. Sci. Food Agric.* **2019**, *99*, 499–506. [[CrossRef](#)]

132. Mourtzinou, I.; Konteles, S.; Kalogeropoulos, N.; Karathanos, V.T. Thermal oxidation of vanillin affects its antioxidant and antimicrobial properties. *Food Chem.* **2009**, *114*, 791–797. [[CrossRef](#)]
133. Yadav, M.; Pandey, R.; Chauhan, N.S. Catabolic Machinery of the Human Gut Microbes Bestow Resilience Against Vanillin Antimicrobial Nature. *Front. Microbiol.* **2020**, *11*, 588545. [[CrossRef](#)]
134. Schwab, W. Natural 4-hydroxy-2,5-dimethyl-3(2H)-furanone (Furaneol(R)). *Molecules* **2013**, *18*, 6936–6951. [[CrossRef](#)]
135. Prester, L. Biogenic amines in fish, fish products and shellfish: A review. *Food Addit. Contam. Part A Chem. Anal. Control. Expo. Risk Assess* **2011**, *28*, 1547–1560. [[CrossRef](#)]
136. Bogdanovic, T.; Petricevic, S.; Brkljaca, M.; Listes, I.; Pleadin, J. Biogenic amines in selected foods of animal origin obtained from the Croatian retail market. *Food Addit. Contam. Part A Chem. Anal. Control. Expo. Risk Assess* **2020**, *37*, 815–830. [[CrossRef](#)]
137. Alvarez-Elcoro, S.; Enzler, M.J. The macrolides: Erythromycin, clarithromycin, and azithromycin. *Mayo. Clin. Proc.* **1999**, *74*, 613–634. [[CrossRef](#)]
138. Ashraf, A.; Liu, G.; Yousaf, B.; Arif, M.; Ahmed, R.; Irshad, S.; Cheema, A.I.; Rashid, A.; Gulzaman, H. Recent trends in advanced oxidation process-based degradation of erythromycin: Pollution status, eco-toxicity and degradation mechanism in aquatic ecosystems. *Sci. Total Environ.* **2021**, *772*, 145389. [[CrossRef](#)]
139. Harju, K.; Koskela, H.; Kremp, A.; Suikkanen, S.; de la Iglesia, P.; Miles, C.O.; Krock, B.; Vanninen, P. Identification of gymnodimine D and presence of gymnodimine variants in the dinoflagellate *Alexandrium ostenfeldii* from the Baltic Sea. *Toxicon* **2016**, *112*, 68–76. [[CrossRef](#)]
140. Rowdhwal, S.S.S.; Chen, J. Toxic Effects of Di-2-ethylhexyl Phthalate: An Overview. *Biomed. Res. Int.* **2018**, *2018*, 1750368. [[CrossRef](#)]
141. Deigan, K.E.; Ferre-D'Amare, A.R. Riboswitches: Discovery of drugs that target bacterial gene-regulatory RNAs. *Acc. Chem. Res.* **2011**, *44*, 1329–1338. [[CrossRef](#)] [[PubMed](#)]
142. Born, J.; Weitzel, K.; Suess, B.; Pfeifer, F. A Synthetic Riboswitch to Regulate Haloarchaeal Gene Expression. *Front. Microbiol.* **2021**, *12*, 696181. [[CrossRef](#)] [[PubMed](#)]
143. Topp, S.; Reynoso, C.M.; Seeliger, J.C.; Goldlust, I.S.; Desai, S.K.; Murat, D.; Shen, A.; Puri, A.W.; Komeili, A.; Bertozzi, C.R.; et al. Synthetic riboswitches that induce gene expression in diverse bacterial species. *Appl. Environ. Microbiol.* **2010**, *76*, 7881–7884. [[CrossRef](#)] [[PubMed](#)]
144. Lotz, T.S.; Suess, B. Small-Molecule-Binding Riboswitches. *Microbiol. Spectr.* **2018**, *6*, RWR-0025-2018. [[CrossRef](#)]
145. Groher, F.; Bofill-Bosch, C.; Schneider, C.; Braun, J.; Jager, S.; Geissler, K.; Hamacher, K.; Suess, B. Riboswitching with ciprofloxacin-development and characterization of a novel RNA regulator. *Nucleic Acids Res.* **2018**, *46*, 2121–2132. [[CrossRef](#)]
146. Boussebayle, A.; Torka, D.; Ollivaud, S.; Braun, J.; Bofill-Bosch, C.; Dombrowski, M.; Groher, F.; Hamacher, K.; Suess, B. Next-level riboswitch development-implementation of Capture-SELEX facilitates identification of a new synthetic riboswitch. *Nucleic Acids Res.* **2019**, *47*, 4883–4895. [[CrossRef](#)]
147. Mally, A.; Solfrizzo, M.; Degen, G.H. Biomonitoring of the mycotoxin Zearalenone: Current state-of-the art and application to human exposure assessment. *Arch. Toxicol.* **2016**, *90*, 1281–1292. [[CrossRef](#)]
148. Liew, W.P.; Mohd-Redzwan, S. Mycotoxin: Its Impact on Gut Health and Microbiota. *Front. Cell. Infect. Microbiol.* **2018**, *8*, 60. [[CrossRef](#)]
149. Saber, T.M.; Abd El-Aziz, R.M.; Ali, H.A. Quercetin mitigates fenitrothion-induced testicular toxicity in rats. *Andrologia* **2016**, *48*, 491–500. [[CrossRef](#)]